

# Changes in Ozone Chemical Sensitivity in the United States from 2007 to 2016

Shannon Koplitz,\* Heather Simon, Barron Henderson, Jennifer Liljegren, Gail Tonnesen, Andrew Whitehill, and Benjamin Wells



Cite This: *ACS Environ. Au* 2022, 2, 206–222



Read Online

ACCESS |

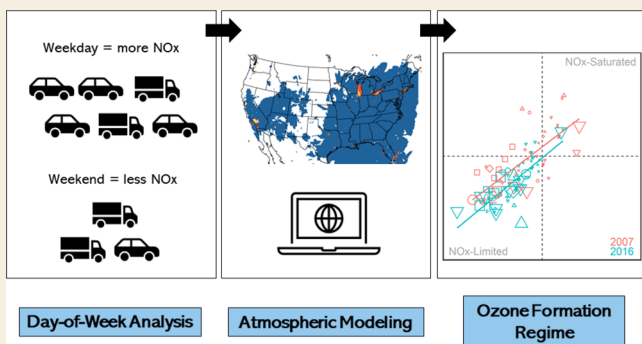
Metrics & More

Article Recommendations

Supporting Information

**ABSTRACT:** Anthropogenic nitrogen oxide ( $\text{NO}_x$ ) and volatile organic compound (VOC) emissions in the United States have declined substantially over the last decade, altering the  $\text{NO}_x$ -VOC chemistry and ozone ( $\text{O}_3$ ) production characteristics of many areas. In this work, we use multiple air quality analysis tools to assess how these large reductions in  $\text{NO}_x$  and VOC have affected  $\text{O}_3$  production regimes across the United States between 2007 and 2016. We first compare observed and modeled evolution of  $\text{NO}_x$ -limited and  $\text{NO}_x$ -saturated  $\text{O}_3$  formation regimes using a day-of-week (DOW) analysis. This comparison builds confidence in the model's ability to qualitatively capture  $\text{O}_3$  changes due to chemistry and meteorology both within years and across periods of large emission decreases. DOW analysis, however, cannot definitively differentiate between emissions and meteorology impacts. We therefore supplement this analysis with sensitivity calculations from the Comprehensive Air Quality Model with Extensions higher-order decoupled direct method (CAMx HDDM) to characterize modeled shifts in  $\text{O}_3$  formation chemistry between 2007 and 2016 in different regions of the United States. We also conduct a more detailed investigation of the  $\text{O}_3$  chemical behavior observed in Chicago and Detroit, two complex urban areas in the Midwest. Both the ambient and modeling data show that more locations across the United States have shifted toward  $\text{NO}_x$ -limited regimes between 2007 and 2016. The model-based HDDM sensitivity analysis shows only a few locations remaining  $\text{NO}_x$ -saturated on high- $\text{O}_3$  days in 2016, including portions of New York City, Chicago, Minneapolis, San Francisco, and Los Angeles. This work offers insights into the current state of  $\text{O}_3$  production chemistry in large population centers across the United States, as well as how  $\text{O}_3$  chemistry in these areas may evolve in the future.

**KEYWORDS:** ozone, chemical sensitivity, U.S. air quality, nitrogen oxide emissions



## 1. INTRODUCTION

Tropospheric ozone ( $\text{O}_3$ ), a respiratory irritant and greenhouse gas that is harmful to human and environmental health, is a secondary air pollutant formed from nitrogen oxides ( $\text{NO}_x$ ) and volatile organic compounds (VOCs) reacting in the presence of sunlight.  $\text{O}_3$  formation can be limited by either precursor. In  $\text{NO}_x$ -limited regimes, reducing  $\text{NO}_x$  concentrations through emission control strategies will effectively lower  $\text{O}_3$  pollution levels. However, highly concentrated  $\text{NO}_x$  emissions (e.g., power plant plumes or automobile traffic in dense urban areas) or uncondusive meteorology (i.e., lower levels of solar radiation) can lead to  $\text{NO}_x$ -saturated (also called VOC-limited or radical-limited)  $\text{O}_3$  formation conditions.<sup>1,2</sup> Under these conditions, reducing VOC concentrations will effectively lower  $\text{O}_3$  pollution levels, while reducing  $\text{NO}_x$  concentrations may cause local increases in  $\text{O}_3$ , although these increases may be reversed with large enough  $\text{NO}_x$  reductions. Responsiveness to local  $\text{NO}_x$  reductions is also dependent on regional emission and transport patterns, for

example, areas downwind of large urban areas will experience some  $\text{O}_3$  formation due to  $\text{NO}_x$  outflow.

Anthropogenic  $\text{NO}_x$  emissions in the United States have decreased significantly since the 1990s due largely to emission control policies enacted by the U.S. Environmental Protection Agency (U.S. EPA).<sup>3,4</sup> Total anthropogenic VOC emissions have also decreased over this period,<sup>3,4</sup> although trajectories vary for individual VOC sources.<sup>5</sup> In addition, biogenic sources contribute the majority of VOC emissions in some locations.<sup>6</sup> These large changes in precursor emissions have substantially altered the relative abundance of  $\text{NO}_x$  and VOC—and therefore the characteristics of  $\text{O}_3$  formation—in some areas

Received: August 27, 2021

Revised: December 1, 2021

Accepted: December 1, 2021

Published: December 16, 2021



with persistent  $O_3$  pollution issues. Understanding the state of  $O_3$  production chemistry across the country informs ongoing air quality management efforts and emission control strategy development at local, regional, and national scales.

Although  $O_3$  formation is and has historically been  $NO_x$ -limited across most of the United States,<sup>7–9</sup> some urban areas have exhibited  $NO_x$ -saturated behavior because of a combination of high localized anthropogenic  $NO_x$  emissions and meteorology.<sup>10–12</sup> While continued reduction of local  $NO_x$  emissions will eventually drive areas with  $NO_x$ -saturated behavior toward  $NO_x$ -limitation,<sup>13,8</sup>  $NO_x$ -saturated conditions dampen the responsiveness of local  $O_3$  formation to local  $NO_x$  emission controls in the near term, presenting complex scenarios for air quality managers.<sup>14</sup> Practical challenges related to the cost of additional emission controls are also an important consideration driving air quality control strategy development. Initially, decreases in  $NO_x$  emissions were largely achieved from mobile sources and power plants (ref 3 and references therein). As precursor emissions are reduced, developing strategies to achieve the additional emission reductions needed for some areas to comply with the  $O_3$  National Ambient Air Quality Standards (NAAQS) becomes more of a challenge scientifically and financially.<sup>15</sup>

Substantial reductions in  $NO_x$  and VOC emissions across the United States over the last few decades and their implications for  $O_3$  air quality have been an ongoing area of research since these changes began to manifest in the atmosphere.<sup>3,8,16–20</sup> Day-of-week (DOW) analysis is a commonly used approach for characterizing shifts in  $O_3$  production because of changes in  $NO_x$  emissions, resulting from weekly traffic patterns.<sup>21–29</sup> Specifically, Marr and Harley<sup>28,29</sup> showed in California that while gasoline vehicle traffic, which emits both  $NO_x$  and VOCs, changed little on weekends, diesel vehicle traffic, which chiefly emits  $NO_x$ , showed a marked decrease on weekends. This type of study provides the opportunity to observe whether  $O_3$  increases or decreases under real-world conditions, for which  $NO_x$  but not VOC emissions have a distinct weekly cycle. These studies generally interpret  $O_3$  increases (as a result of  $NO_x$  decreases) on weekends versus weekdays, barring any systematic meteorological differences, as an indication of  $NO_x$ -saturated chemical conditions. Conversely, when  $O_3$  decreases along with  $NO_x$  on weekends versus weekdays, it may be an indication of  $NO_x$ -limited chemical conditions.

One limitation of observationally based DOW analysis is the inability to distinguish influences of changes in meteorology<sup>30</sup> compared to changes in emissions on  $O_3$  chemistry.<sup>30</sup> Although air quality models are prone to uncertainties and experience their own sets of limitations, these tools can more clearly differentiate the relative effects of emissions and meteorology on pollutant concentrations. For example, Koo et al.<sup>31</sup> used air quality modeling to characterize weekend  $O_3$  effects in the Midwestern United States during summer 2005 and, after accounting for meteorology, attributed the differences to lower  $NO_x$  emissions on weekends. Air quality models can also characterize  $O_3$  chemistry in areas not covered as densely by surface monitors; for example, Jin et al.<sup>8</sup> used the GEOS-Chem global chemical transport model and satellite data from the ozone monitoring instrument to assess changes in  $O_3$  formation regimes from 2005 to 2015 across multiple regions in China, Europe, and the United States.

Here, we build on Jin et al.<sup>8</sup> and the other work mentioned above by continuing to investigate how trends in precursor

emissions affect  $O_3$  formation regimes across the United States. To this end, we use a high-resolution regional air quality model implemented with the higher-order decoupled direct method (HDDM) along with surface monitoring observations to identify changes in  $O_3$  formation chemistry between 2007 and 2016. The HDDM tool allows for the calculation of  $O_3$  sensitivities to its chemical precursors in all grid cells throughout a simulation. We first compare model-based characterizations of  $O_3$  formation regimes derived from daily modeled  $O_3$  concentrations at specific locations against available surface observations through a DOW analysis. We then use the HDDM sensitivities obtained from the model to isolate the model-predicted impact of emissions alone on  $O_3$  formation chemistry and to estimate more broadly how  $O_3$  formation regimes have changed nationally between 2007 and 2016.

## 2. METHODS

### 2.1. CAMx HDDM Simulations

We applied the Comprehensive Air Quality Model with Extensions (CAMx) v6.5<sup>32</sup> with a 12 km spatial resolution over the contiguous United States for two full calendar years, 2007 and 2016, including a 10-day spin-up period that was not used in the analysis (e.g., December 22, 2015 to December 31, 2016). Anthropogenic emission inputs came from the National Emission Inventory (NEI)-based platforms for 2007<sup>33</sup> and 2016.<sup>34</sup> Nationally,  $NO_x$  emissions from anthropogenic sources and fires decreased by 39% between the 2007 modeled inventory and the 2016 modeled inventory (Table S1). Nationally, modeled VOC emissions changed little between the 2 years, but this was due to substantial heterogeneity at the state level with some states estimated to have large increases in VOC emissions and others estimated to have large decreases (Table S1). Meteorological inputs, including horizontal wind speed and direction, temperature, moisture, vertical diffusion rates, and rainfall rates, were archived from the Weather Research and Forecasting model (WRF)<sup>35,36</sup> and implemented into CAMx. Initial and boundary conditions were created using the GEOS-Chem model<sup>37</sup> for 2007 and the hemispheric version of Community Multiscale Air Quality (CMAQ) modeling system<sup>38</sup> for 2016. More details about specific inputs and model configuration options are described in the reference documentation for the 2015 (Chapter 4 Appendix)<sup>39</sup> and 2020<sup>40</sup>  $O_3$  NAAQS reviews. Model performance evaluations were also previously conducted for both 2007 and 2016 emission platforms as part of the 2015<sup>39</sup> and 2020<sup>40</sup>  $O_3$  NAAQS reviews, respectively.

CAMx was run using the HDDM tool, which calculates in-model sensitivities of model outputs to an input or model parameter, for example,  $O_3$  concentrations to  $NO_x$  emissions, and is well suited for source-oriented studies.<sup>41,42</sup> HDDM has previously been applied in regional air quality modeling studies by the U.S. EPA for policy-relevant assessments.<sup>39,40</sup> Both first- and second-order sensitivities were tracked using the HDDM for the relationship between  $O_3$  and U.S. anthropogenic  $NO_x$ . First-order sensitivities were tracked using the HDDM for the relationship between  $O_3$  and U.S. anthropogenic VOC emissions. Emission sectors included as U.S. anthropogenic were agriculture, commercial marine vessels, fugitive dust, onroad and nonroad mobile, point sources, nonpoint, rail, and residential wood combustion. Biogenics—calculated with the Biogenic Emissions Inventory System<sup>43</sup>—fires, and sources from Canada and Mexico were not counted as U.S. anthropogenic emissions in this analysis. HDDM sensitivities represent the change at the grid cell from both local  $O_3$  production sensitivity and the transport history of the air arriving at the grid cell.

### 2.2. DOW Analysis

A DOW assessment was undertaken to build confidence in the model's utility for characterizing  $O_3$  formation regimes. As discussed above, differences in weekend versus weekday  $O_3$  values have

previously been used to assess whether areas are  $\text{NO}_x$ -limited or  $\text{NO}_x$ -saturated. In this assessment, we compare weekend/weekday patterns between the model and the observations for the U.S. nonattainment areas (areas designated nonattainment for the 2015  $\text{O}_3$  NAAQS) and examine the changes in these patterns between 2007 and 2016.

Maximum daily 8 h average (MDA8)  $\text{O}_3$  values were calculated from 2007 to 2016  $\text{O}_3$  monitor data available through EPA's air quality system (AQS), as described in 40 CFR Appendix P to Part 50 ([https://www.ecfr.gov/cgi-bin/text-idx?tpl=/ecfrbrowse/Title40/40cfr50\\_main\\_02.tpl](https://www.ecfr.gov/cgi-bin/text-idx?tpl=/ecfrbrowse/Title40/40cfr50_main_02.tpl)). MDA8  $\text{O}_3$  values were also calculated from the gridded hourly 2007 and 2016 model results using the same methodology. Modeled MDA8  $\text{O}_3$  values were extracted for grid cells that contained an  $\text{O}_3$  monitoring site. Modeled and observed MDA8  $\text{O}_3$  values paired in space and time were used to compare DOW patterns. For this analysis, we eliminate "transition" days between weekends and weekdays in order to avoid multiday impacts that could obscure differences between weekdays and weekends. To this end, only Sundays were categorized as weekend days, and Tuesdays, Wednesdays, and Thursdays were categorized as weekdays. For each nonattainment area, weekend and weekday  $\text{O}_3$  distributions during May–September were compared for modeled and measured MDA8 values in 2007 and 2016. Valid data from all monitoring sites within each nonattainment area were included in the comparison with no spatial averaging. We also explored using data from individual monitors rather than aggregating across nonattainment areas, but found that using single monitor data generally leads to insignificant results due to small sample sizes.

Welch's t-tests were performed on each set of data to determine whether MDA8 values were statistically different ( $p < 0.05$ ) between weekends and weekdays. T-test  $p$ -values are valid even for very small sample sizes.<sup>44</sup> Welch's t-test is also preferred for unequal sample sizes, as is the case for the weekend vs weekday datasets in our DOW analysis. However, Welch's t-test can result in diminished statistical power at lower sample sizes. We therefore have also included results from a Monte Carlo analysis for several of the largest urban areas (Atlanta, Chicago, Houston, and Los Angeles) in the Supporting Information (Figures S1–S4) that shows our significance results are robust against randomizing the observations of which are included.

We label areas with statistically higher distributions of MDA8  $\text{O}_3$  on weekends as " $\text{NO}_x$ -saturated". Conversely, we label areas with statistically lower distributions of MDA8  $\text{O}_3$  on weekends as " $\text{NO}_x$ -limited". Areas where the t-test returns a  $p$ -value  $>0.05$  are labeled as "mixed" sensitivity or transitional chemical regimes.

### 2.3. HDDM-Based Assessment of Chemical Sensitivity

CAMx HDDM results were used to calculate changes in MDA8  $\text{O}_3$  that would occur with perturbations in the U.S. anthropogenic  $\text{NO}_x$  and/or VOC using eq 1.

$$\begin{aligned} \Delta\text{MDA8}(\text{dNO}_x, \text{dVOC}) &= \text{dNO}_x S_{\text{NO}_x}^{(1)} + \left( \frac{\text{dNO}_x^2}{2} \right) S_{\text{NO}_x}^{(2)} + \text{dVOC} S_{\text{VOC}}^{(1)} \\ &\quad + \left( \frac{\text{dNO}_x \text{dVOC}}{2} \right) S_{\text{NO}_x, \text{VOC}}^{(2)} \end{aligned} \quad (1)$$

Equation 1 calculates the change in MDA8 ( $\Delta\text{MDA8}$ ) as a function of fractional changes in  $\text{NO}_x$  or VOC ( $\text{dNO}_x$  or  $\text{dVOC}$ ) using sensitivity parameter ( $S$ ). For this run, the HDDM was configured to store first-order sensitivities for  $\text{NO}_x$  and VOC ( $S^{(1)}_{\text{NO}_x}$ ,  $S^{(1)}_{\text{VOC}}$ ), second-order sensitivity to  $\text{NO}_x$  ( $S^{(2)}_{\text{NO}_x}$ ), and the interaction between  $\text{NO}_x$  and VOC ( $S^{(2)}_{\text{NO}_x, \text{VOC}}$ ). Equation 1 is applied for each monitor and day with day- and location-specific sensitivity parameters from the HDDM. HDDM outputs hourly data by default, which have been averaged over the 8 h MDA8 period for each day and location. For VOC-only changes, the first, second, and fourth terms are zero. For  $\text{NO}_x$ -only emission changes, the third and fourth terms are zero. As such, 20% reductions in either emission independently can be simplified, as shown in eqs 2 and 3.

$$\Delta\text{MDA8}_{-20\text{NO}_x} = -0.2S_{\text{NO}_x}^{(1)} + \left( \frac{(-0.2)^2}{2} \right) S_{\text{NO}_x}^{(2)} \quad (2)$$

$$\Delta\text{MDA8}_{-20\text{VOC}} = -0.2S_{\text{VOC}}^{(1)} \quad (3)$$

Based on the results from Simon et al.<sup>45</sup> (Figure 4), the calculated  $\Delta\text{MDA8}$  scales linearly for emission reductions lower than 20%, assuming that substantially larger emission reductions could introduce nonlinearities.

$\Delta\text{MDA8}_{-20\text{NO}_x}$  and  $\Delta\text{MDA8}_{-20\text{VOC}}$  were used to characterize each day and grid cell into three categories using criteria from Jin et al.<sup>8</sup>  $\text{NO}_x$ -limited,  $\text{NO}_x$ -saturated, and mixed:

- $\text{NO}_x$ -limited:  $\Delta\text{MDA8}_{-20\text{NO}_x} < 0$  and  $|\Delta\text{MDA8}_{-20\text{NO}_x}| > |\Delta\text{MDA8}_{-20\text{VOC}}|$
- $\text{NO}_x$ -saturated:  $\Delta\text{MDA8}_{-20\text{NO}_x} > 0$
- Mixed:  $\Delta\text{MDA8}_{-20\text{NO}_x} < 0$  and  $|\Delta\text{MDA8}_{-20\text{NO}_x}| < |\Delta\text{MDA8}_{-20\text{VOC}}|$

Here, " $\text{NO}_x$ -limited" does not necessarily imply lack of responsiveness to VOC reductions, just stronger responsiveness to  $\text{NO}_x$  reductions. We define " $\text{NO}_x$ -saturated" regimes as showing an  $\text{O}_3$  disbenefit to  $\text{NO}_x$ . Finally,  $\text{O}_3$  in "mixed" regimes responds to reductions of both  $\text{NO}_x$  and VOC, but responds more strongly to VOC than  $\text{NO}_x$ . Chemical regimes were then mapped using varying averaging periods and MDA8  $\text{O}_3$  threshold values.

### 2.4. Development of $\text{O}_3$ Isopleths

We developed  $\text{O}_3$  isopleth diagrams based on the HDDM results described above for select locations. These diagrams allow for the visualization of  $\text{O}_3$  isopleths as a function of VOC (x-axis) and  $\text{NO}_x$  (y-axis) concentrations. To build the  $\text{O}_3$  isopleths, eq 1 is applied to calculate daily  $\text{O}_3$  isopleths for all days above a threshold value (e.g., MDA8  $> 70$  ppb) for a matrix of emission changes ( $-100$  to  $+50\%$ ) for  $\text{NO}_x$  and VOC. The change in MDA8 for each day is added to the original MDA8 to construct the  $\text{O}_3$  isopleths in total MDA8 space instead of change. The daily  $\text{O}_3$  isopleths are then averaged to produce a representative diagram.

The diagrams referred to here as  $\text{O}_3$  isopleths are similar to plots associated with the empirical kinetic modeling approach (EKMA). EKMA relates the initial VOC and  $\text{NO}_x$  concentrations to levels of  $\text{O}_3$  production in one-dimensional (1D) kinetic box models.<sup>46</sup> By varying the initial conditions for the box model,  $\text{O}_3$  isopleths were created and then related to observed (empirical)  $\text{O}_3$  maxima; these isopleths were sometimes referred to as EKMA diagrams (e.g., ref 47). Our  $\text{O}_3$  isopleths relate daily maximum  $\text{O}_3$  concentration to domain-wide U.S. anthropogenic  $\text{NO}_x$  and VOC emissions using the HDDM). This explicitly calculates the sensitivity of  $\text{O}_3$  to domain-wide emissions, which has then been added to the original concentrations to generate the isopleths. Plotting  $\text{O}_3$  concentration as a function of emission levels<sup>48,49</sup> (e.g., refs 48 and ref 49) rather than the more traditional  $\text{O}_3$  production as a function of precursor concentrations makes these figures more directly applicable to air quality planning as it provides information on what level of  $\text{NO}_x$  and VOC emissions are necessary to reach target  $\text{O}_3$  concentrations in an area.

We note that while  $\text{O}_3$  isopleths were constructed to show  $\text{O}_3$  values at  $\text{NO}_x$  and VOC emission levels between 0 and 150% of the modeled emission levels ( $-100\%$ ,  $+50\%$ ), past studies have suggested that the HDDM estimates become increasingly uncertain when applied to emission changes of more than 50%.<sup>45,50</sup> We therefore caution that  $\text{O}_3$  predictions displayed below 50%  $\text{NO}_x$  and VOC emission levels are highly uncertain.

Additionally, the  $\text{O}_3$  isopleth diagrams do not assume a relationship between the production of  $\text{O}_3$  and  $\text{O}_3$  levels. Instead, they calculate the sensitivity of  $\text{O}_3$  levels to anthropogenic U.S. emissions based on the HDDM results, which are calculated within the model by taking partial derivatives of the governing equations. The HDDM sensitivities for a specific grid cell and time-step therefore incorporate the impacts of all modeled physical and chemical processes across the model domain that have impacted that modeled  $\text{O}_3$  concentration since the beginning of the model simulation. These diagrams,

therefore, make no assumptions about where  $O_3$  is produced. Because the  $O_3$  isopleths are derived from the HDDM applied at a national scale, the changes in any location incorporate the impact of both local production and  $O_3$  transport. The portion of the  $O_3$  isopleths that is insensitive to emission changes inherently accounts for both the lateral boundary conditions and the in-domain sources that are not U.S. anthropogenic. When local  $O_3$  concentrations are meaningfully above “background” concentrations, the local production will tend to dominate the response. In cases where background sources dominated the simulated  $O_3$ , the isopleth would show little variability. We, therefore, focus on MDA8 and the top 10 days. When these days are insensitive to U.S.- $NO_x$  and U.S.-VOC, they may conceptually still be sensitive to background sources.

### 3. RESULTS

We present results from the DOW analysis and HDDM calculations for consideration as complementary pieces of information, rather than opposing methods to be compared. The DOW analysis provides an observationally based characterization of  $O_3$  changes, as well as an opportunity to evaluate the model-simulated DOW differences, but cannot separate the influence of emissions and/or chemistry from meteorological patterns. The HDDM results allow for the explicit calculation of  $O_3$  chemical sensitivity, but cannot confirm the real-world fidelity of these relationships.

#### 3.1. DOW Analysis

We start by examining the observed and modeled weekend versus weekday MDA8  $O_3$  values for May through September days. In Figure 1, we show distributions of MDA8  $O_3$  on



**Figure 1.** May–September weekday versus weekend MDA8  $O_3$  concentrations in the Chicago nonattainment area for 2007 and 2016 based on monitored values (left panel) and on modeled values in grid cells containing monitor locations (right panel). Boxes represent the 25th–75th percentile, horizontal lines represent median values, whiskers extend to 1.5× the interquartile range, dots show outlier values, and triangles represent 95th percentile values. Boxplot pairs that have statistically different mean values on weekends versus weekdays are outlined in bold.

weekends and weekdays in the Chicago nonattainment area during 2007 and 2016. The Chicago nonattainment area includes Cook County as well as the surrounding counties in Illinois, Indiana, and Wisconsin. Welch's t-test shows that the mean observed MDA8  $O_3$  concentrations on weekends are not statistically different than the mean on weekdays in 2007 but are statistically lower than the mean on weekdays across all observed values in 2016. This suggests that the Chicago metropolitan area as a whole exhibited a mixed chemical regime in 2007 and was  $NO_x$ -limited in 2016. This metric looks across all measured values and includes MDA8  $O_3$  both at locations inside and outside of the urban core and on

summer days with low measured  $O_3$  values. When looking only at the 95th percentile observed MDA8  $O_3$  values, Figure 1 shows lower MDA8  $O_3$  on weekends than on weekdays in both 2007 and 2016, although it is not possible to quantify whether this single value is statistically different. The modeled values in the Chicago metro area are statistically higher on weekends versus weekdays in the 2007 simulation and are statistically lower on weekends versus weekdays in 2016. Therefore, while both the modeled and the measured mean MDA8  $O_3$  values in Chicago are higher on weekends compared to weekdays in 2007, the difference is only statistically significant in the model, suggesting that the simulated conditions in Chicago are more strongly  $NO_x$ -saturated than the observed conditions. Both model and observations suggest a statistically significant shift to  $NO_x$ -limited conditions in 2016.

Spatial differences within the Chicago area are demonstrated in Figures S5 and S6, which show monitor-level boxplots for the suburban Northbrook monitor in Cook County, IL, and another monitor in an industrial area of Indiana (Gary). The t-test results for data from a single monitor are not statistically significant at either of these sites, likely due to the smaller sample size of data compared to pooling data from the entire nonattainment area. Nonetheless, qualitative comparisons of the plots are informative. For 2007, observed data at the Northbrook monitor show higher mean MDA8 values on weekends than weekdays, suggesting  $NO_x$ -saturated conditions. In contrast, 2007 observations at Gary show lower mean MDA8  $O_3$  values on weekends compared to weekdays, suggesting  $NO_x$ -limited conditions. In 2016, the ambient data at both monitors have lower mean  $O_3$  on weekends than on weekdays, suggesting a shift toward  $NO_x$ -limited conditions. In Section 3.3, we further investigate spatial heterogeneity within both the Chicago and Detroit nonattainment areas.

In Figures 2 and 3, we look more broadly across the United States at the model's capability of simulating both weekend–weekday (WE–WD) patterns and the change in these patterns between 2007 and 2016. Figure 2 focuses on changes in the 95th percentile MDA8  $O_3$  with larger positive values representing more  $NO_x$ -saturated conditions and larger negative values representing more  $NO_x$ -limited conditions. Here, we do not define a quantitative cut point to delineate when the positive or negative WE–WD differences are significantly different from zero. Whereas in Figure 3, we look across all May–September days at all monitor locations within each nonattainment area and use Welch's t-test with  $p$ -values  $<0.05$  to characterize which nonattainment areas have statistically different weekday and weekend MDA8  $O_3$  values as described in Section 2.2. We then plot how the measured and modeled WE–WD differentials have changed by region between 2007 and 2016. The data underlying Figure 3 and the associated chemical regime category for each nonattainment area based on Welch's t-test results are provided in Table S2. Figures 2 and 3 show that the model is generally skilled at simulating relative weekend versus weekday differences as well as changes in the weekend effect between 2007 and 2016. Modeled chemical regime characterizations based on WE–WD differences match monitor-based characterizations in 33 out of 49 nonattainment areas in 2007 and 40 out of 49 nonattainment areas in 2016 (Table S2). All but one of the cases that do not match involve either a model or observed characterization of a “mixed” chemical regime. In other words, there is only a single case (Los Angeles in 2016) where the model predicts

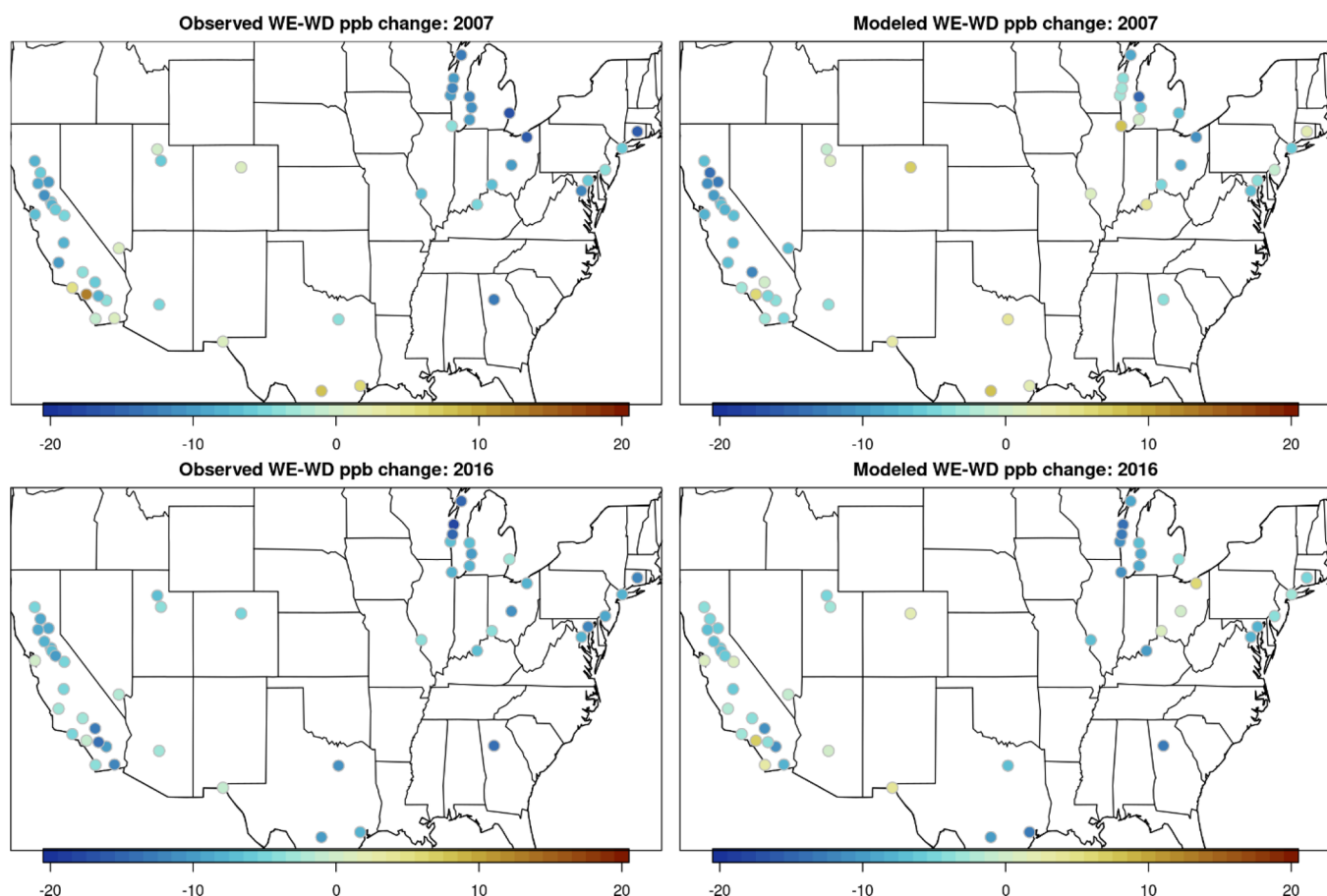


**Figure 2.** Absolute difference (ppb) in May–September 95th percentile nonattainment area MDA8 O<sub>3</sub> values on WE–WD based on monitored values (left panels) and modeled values (right panels) in 2007 (top panels) and 2016 (bottom panels). Each dot represents a single nonattainment area. Data from all monitoring sites within each nonattainment area are pooled to determine the 95th percentile values. Note that the Uintah Basin is not represented in this plot because high O<sub>3</sub> values for this nonattainment area are not observed during May–September.

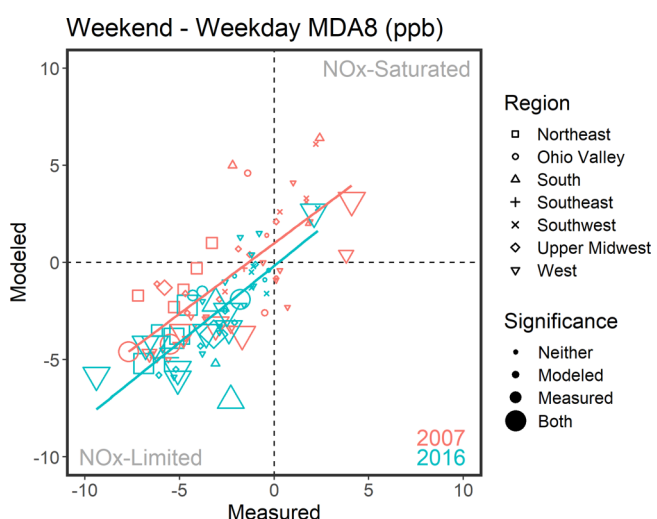


**Figure 3.** Measured vs modeled WE–WD differences in nonattainment areas by region in 2007 and 2016. The size of the shape corresponds to whether neither, one, or both values were highly significant (i.e.,  $p$ -value less than 0.01). See Table S2 for specific areas and WE–WD values.

NO<sub>x</sub>-saturated conditions and the monitor data predict NO<sub>x</sub>-limited data (or vice versa). All other cases where characterizations of chemical regimes do not match are due to the

difference being statistically insignificant in either the model or monitor data.

The modeling presented here was conducted using 12 km spatial resolution and is intended to represent a national-scale domain. It is not surprising that 12 km modeling cannot fully capture O<sub>3</sub> formation regimes in Los Angeles, which is impacted by large spatial gradients in emission sources as well as complex terrain which generally requires a finer grid to properly resolve. Although in this analysis the CAMx modeling system was able to at least qualitatively capture observed WE–WD transitions in other major urban areas across the country like New York, Chicago, and Houston, this lack of fidelity at the 12 km scale remains a limitation to fully resolving atmospheric features in many of these other complex urban landscapes as well.

At a national scale, both the observations and the model suggest that the United States has moved toward more NO<sub>x</sub>-limited O<sub>3</sub> formation chemistry between 2007 and 2016, likely due to substantial NO<sub>x</sub> emission reductions that occurred over that time period. The observations suggest that 6 out of 49 of the nonattainment areas were NO<sub>x</sub>-saturated in 2007, while only 1 (San Francisco) was NO<sub>x</sub>-saturated in 2016. Similarly, the model suggests that the number of NO<sub>x</sub>-saturated nonattainment areas decreased from 11 in 2007 to 2 (San Francisco and Dona Ana, NM) in 2016.

As mentioned above, the analyses shown in Figures 1–3 do not capture spatial heterogeneity within each nonattainment

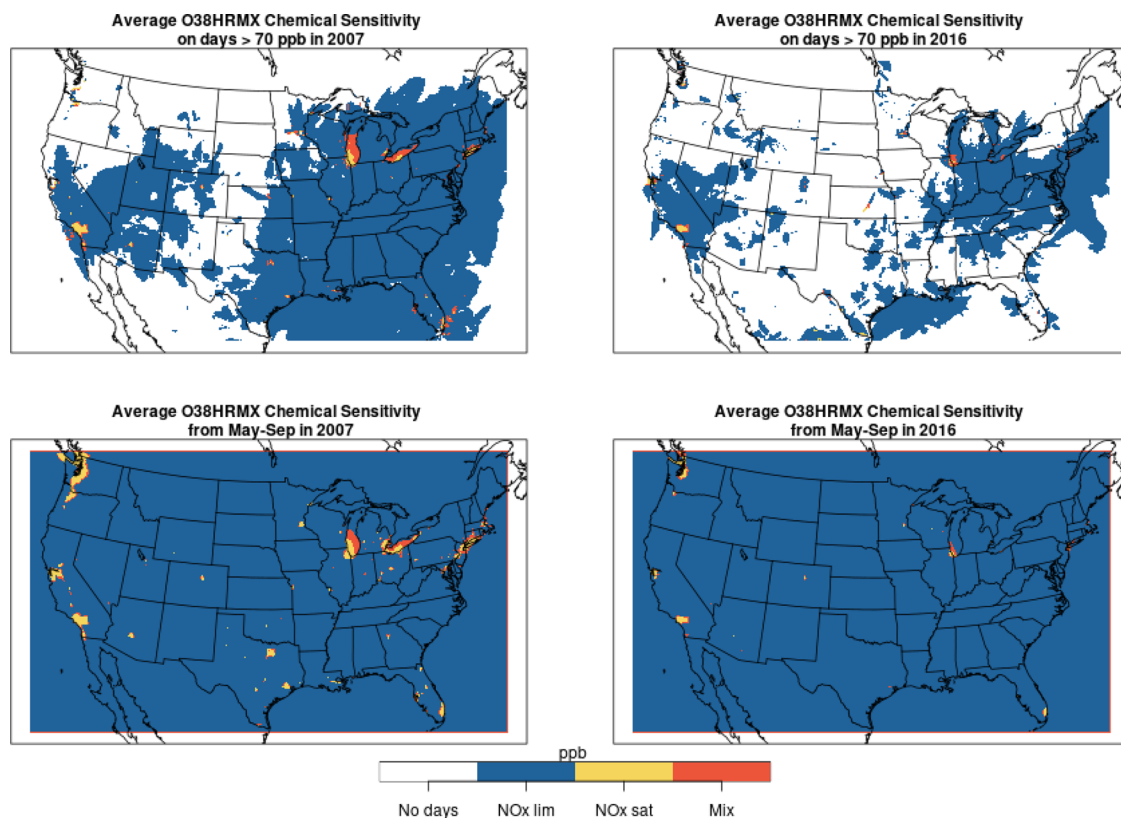


**Figure 4.** Modeled chemical sensitivity by category (see Section 2.3) on days with MDA8 above 70 ppb (top) and all days during May–September (bottom) for 2007 (left panels) and 2016 (right panels).

area. Table S3 provides the DOW results for the monitor with the highest 2016  $O_3$  design value (the regulatory metric which is calculated as the 3 year average of the annual 4th highest MDA8  $O_3$  concentration) within each nonattainment area (the design value for meeting the 2015  $O_3$  NAAQS (or  $O_3$  standard) in the United States is 0.070 ppm truncating the thousandths place (*i.e.* < 71 ppb)). In cases where two monitors within a nonattainment area have the same 2016 design value, both monitors are included in the table. When looking only at data from the highest monitor in each area, most areas are categorized as having a “mixed” chemical regime. This is likely due to the substantially lower sample size when only including data from a single monitor, leading to decreased power of the significance test. Nevertheless, when looking only at the highest monitor, the total number of areas with higher weekend concentrations than weekday concentrations ignoring statistical significance is similar to that determined when including all monitors within the area.

### 3.2. HDDM-Based Assessment of Chemical Sensitivity

In the previous section, we applied DOW methods for determining  $O_3$  formation regimes, which do not account for synoptic-scale changes in meteorology that can result in more favorable  $O_3$  formation conditions on either weekends or weekdays in any particular year,<sup>51</sup> independent of DOW emission patterns. The HDDM capabilities of the CAMx model provide a more direct measure of  $O_3$  formation chemistry within the model. Here, we look at changes in MDA8  $O_3$  predicted with 20% reductions of  $NO_x$  and VOC, respectively, to characterize  $O_3$  formation regimes at each grid cell, as described in Section 2.3.

We start by examining changes in  $O_3$  formation regimes at the national scale (Figure 4). Zoomed-in regional maps are provided in the Supporting Information (Figures S20–S28). The top panels show model-based  $O_3$  formation regimes on days when MDA8  $O_3$  was modeled above 70 ppb, and the bottom panels show  $O_3$  formation regimes averaged over all May–September days. Comparing top and bottom panels in Figure 4 shows that the United States tends to be more  $NO_x$ -limited when looking at high  $O_3$  days than when looking across all days in the  $O_3$  season, as demonstrated by more yellow and orange coverage in the lower two panels than in the upper two panels. This difference between  $O_3$  formation on high days versus the seasonal average is most evident in 2007 in the Eastern United States. This matches with the previous literature that suggests that locations tend to be more  $NO_x$ -saturated on days with less solar radiation and therefore less conducive meteorology for  $O_3$  formation (*e.g.* ref 12). Two major patterns are evident when comparing modeled 2007 and 2016  $O_3$  formation regimes. First, the number of high  $O_3$  days (MDA8 > 70 ppb) has decreased between 2007 and 2016 across the country, as demonstrated by the increasing coverage of white on the top two panels of Figure 4, especially in the Eastern United States. Second, more locations in the United States have transitioned toward  $NO_x$ -limited  $O_3$  formation regimes. While much of the country exhibited primarily  $NO_x$ -limited behavior in 2007, even more of the country exhibited  $NO_x$ -limited behavior by 2016, as demonstrated by the additional coverage of blue in the 2016 maps as well as shifts from  $NO_x$ -saturated (yellow) to mixed (orange) regimes. There are only a handful of areas that demonstrate  $NO_x$ -saturated or mixed formation regimes in 2007, and in Figures 5

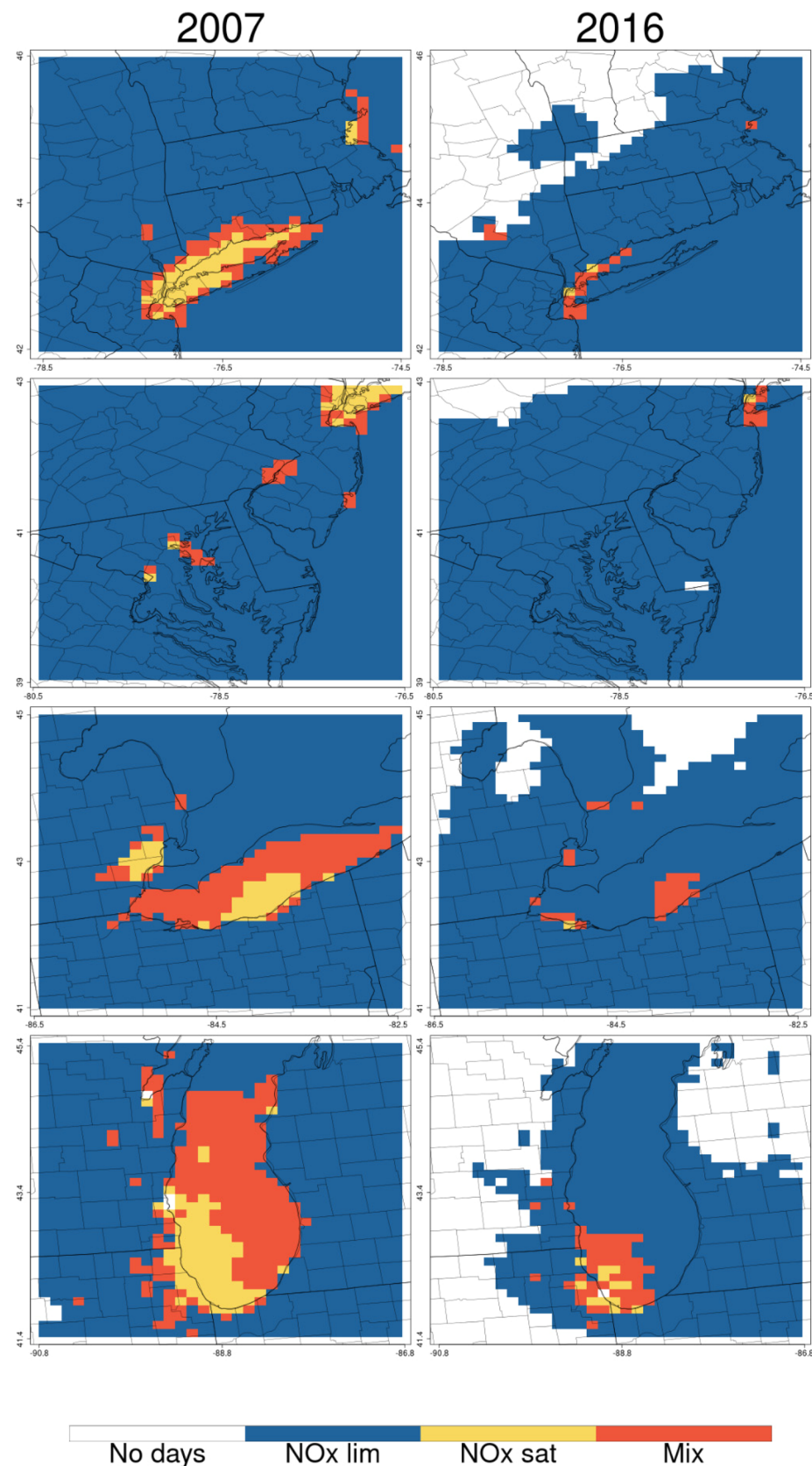


**Figure 5.** Chemical sensitivity on days above 70 ppb in select regions of the Eastern United States in 2007 (left side) and 2016 (right side). Focal urban areas: New York City/Boston (top), Baltimore/Washington DC (second), Detroit (third), and Chicago (bottom).

and 6, we more closely examine several of these locations in the Eastern and Western United States, respectively.

In Figure 5, we examine  $O_3$  response in the Eastern U.S. on days with modeled MDA8  $O_3 > 70$  ppb. Specifically, we focus

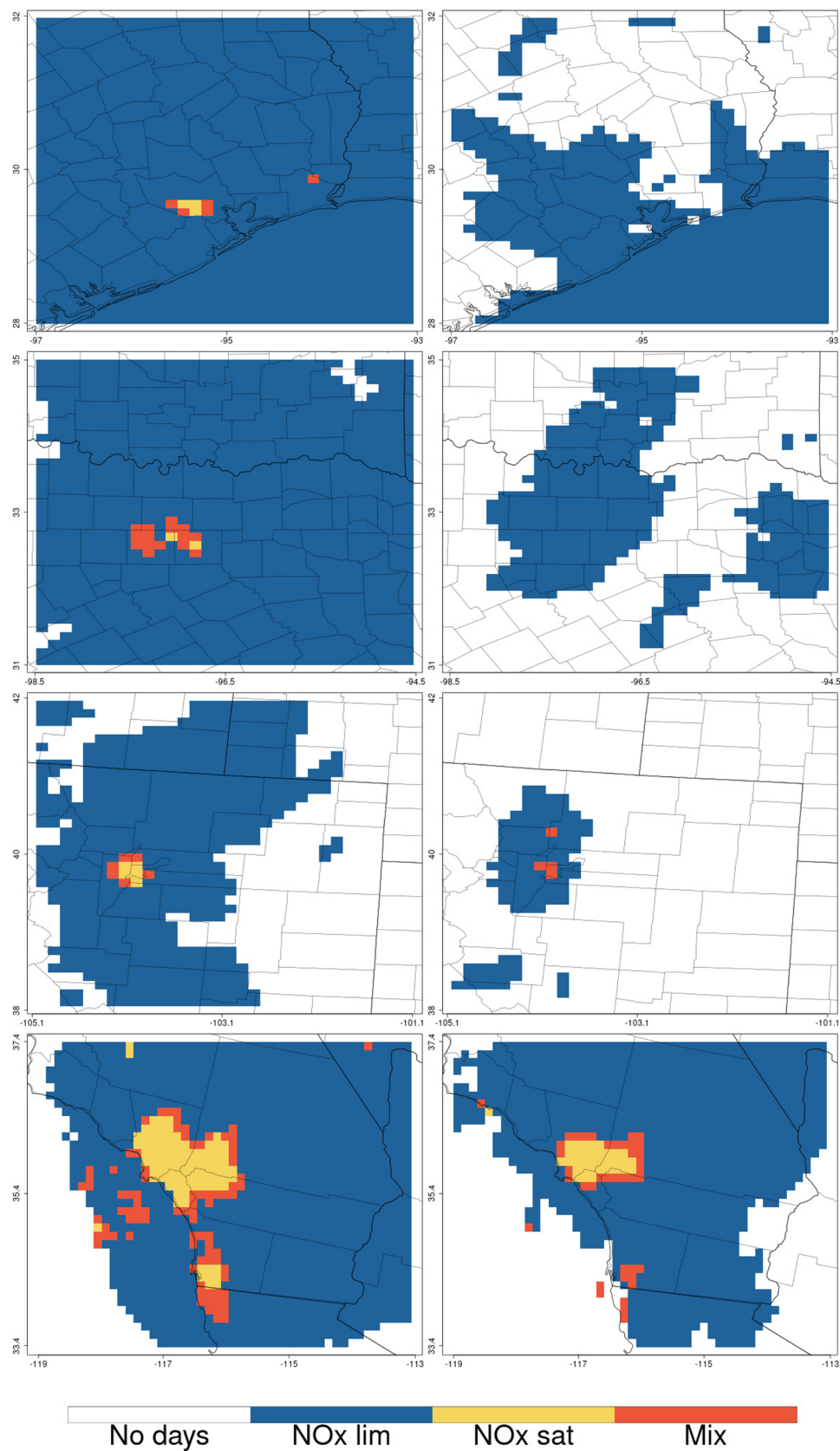


**Figure 6.** Chemical sensitivity on days above 70 ppb in select regions of the Western United States in 2007 (left side) and 2016 (right side). Focal urban areas: Houston (top), Dallas (second), Denver (third), and Los Angeles/San Diego (bottom).

on the regions around New York City, Washington DC, Detroit, and Chicago, areas with historically high  $O_3$  values and

substantial changes in  $NO_x$  and VOC emissions over the past several decades. Based on the model predictions over this time

period, the Northeast has shifted from having  $\text{NO}_x$ -limited conditions in suburban and rural areas and  $\text{NO}_x$ -saturated conditions in most urban areas in 2007 to having  $\text{NO}_x$ -limited conditions almost everywhere in 2016. On high  $\text{O}_3$  days, across the Northeast corridor in 2016, there are only two grid cells, both in New York City, that are still predicted to have  $\text{NO}_x$ -saturated conditions, while the Baltimore, Washington DC, Philadelphia, and Boston metro areas are predicted to be entirely  $\text{NO}_x$ -limited. Both the transitional behavior simulated for New York City and the broader regional patterns of  $\text{NO}_x$ -limitation are generally consistent with a previous study.<sup>10</sup> The changes in  $\text{O}_3$  formation regimes along the Lake Michigan and Lake Erie shorelines show similar increases in the spatial extent of locations predicted to be  $\text{NO}_x$ -limited, although there are several remaining  $\text{NO}_x$ -saturated and mixed locations in 2016, especially in the Chicago area.

$\text{O}_3$  production in the Western United States shows similar transitions over major metropolitan areas (Figure 6). High days occurred across much of Texas in 2007 (shown by non-white grid cells in Figure 6). By 2016, there were far fewer high days and those that occurred were confined mainly along the Gulf Coast and over the urban metro areas, likely due to the continued influence of oil and natural gas and onroad vehicle emissions in these locations. The Houston and Dallas urban cores transitioned completely to  $\text{NO}_x$ -limited behavior by 2016. This trend toward  $\text{NO}_x$ -limitation in eastern Texas has also been identified previously.<sup>52</sup> The spatial extent of locations with MDA8  $\text{O}_3$  above 70 ppb in the Rocky Mountain Front Range decreased substantially between 2007 and 2016, with the model predicting that  $\text{O}_3$  formation regimes in the Denver urban core shifted from  $\text{NO}_x$ -saturated to a mixed regime. Even Los Angeles/Southern California shows a decreased extent of transitional/ $\text{NO}_x$ -saturated behavior, although high  $\text{O}_3$  days persist across the region, and the Los Angeles urban core remains  $\text{NO}_x$ -saturated in the model.

The general pattern displayed in Figures 5 and 6 is also predicted in other regions of the United States. (Figures 4, S20–28). In 2007, there were many urban areas with urban core locations predicted to be  $\text{NO}_x$ -saturated with most other locations predicted to be  $\text{NO}_x$ -limited on high  $\text{O}_3$  days. In 2016, the United States has shifted to being predominantly  $\text{NO}_x$ -limited with only a limited set of cities having any  $\text{NO}_x$ -saturated or mixed chemical regime locations on high  $\text{O}_3$  days. The southeast (Figure S21) is predicted to have no locations with  $\text{NO}_x$ -saturated conditions on high  $\text{O}_3$  days in 2016. Cities with a small  $\text{NO}_x$ -saturated urban core area on high  $\text{O}_3$  days in 2016 include Sandusky Ohio, Chicago, Minneapolis, Omaha, Seattle, San Francisco, and Los Angeles. Some other urban areas are predicted to have some mixed sensitivity locations in their urban cores but no  $\text{NO}_x$ -saturated locations on high  $\text{O}_3$  days: Boston, Miami, Milwaukee, Detroit, Cleveland, Indianapolis, San Antonio, Denver, Sacramento, and San Diego. All other U.S. cities are predicted to be entirely  $\text{NO}_x$ -limited on high  $\text{O}_3$  days. In the urban areas that are predicted to have some remaining locations that are  $\text{NO}_x$ -saturated in 2016, the extent of the  $\text{NO}_x$ -saturated regions has decreased substantially to within a spatially limited core area, typically in the more populous and/or industrialized portions of each area.

We also include figures in the Supporting Information showing how the DOW analysis results quantitatively compare with the HDDM sensitivities for 2007 and 2016 (Figure S41). While the exact relationship varies by monitor, the model-predicted change with a 20% cut in  $\text{NO}_x$  is highly correlated

with modeled WE–WD  $\text{O}_3$  differences, and both methods indicate that HDDM-DOW patterns shift toward  $\text{NO}_x$ -limited behavior between 2007 and 2016.

### 3.3. Case Studies: Chicago and Detroit

We next examine in more detail the chemical behavior of Chicago and Detroit, the two complex urban areas in the Midwest that exhibit predominantly  $\text{NO}_x$ -limited behavior by 2016. We chose to examine Chicago and Detroit more closely because of their large populations—they represent the 5th and 14th most populated cities in the United States, respectively—and coverage during recent field campaigns (Lake Michigan Ozone Study in 2017, Michigan–Ontario Ozone Source Experiment in 2021).

**3.3.1. Chicago.** The Chicago nonattainment area is located adjacent to southern Lake Michigan and consists of portions of Illinois (IL), Indiana (IN), and Wisconsin (WI). High  $\text{O}_3$  episodes around southern Lake Michigan are characterized by high precursor emissions and atmospheric temperature inversions (stagnation) associated with regional high-pressure systems and/or localized land-lake breeze circulations setting up shallow mixing layers.<sup>53,54</sup> Wind directions on high  $\text{O}_3$  days tend to range from southerly to southeasterly and/or southwesterly to westerly.<sup>53,55</sup> Based on 1998–2002 data, ground-based monitoring sites around southern Lake Michigan displayed the weekend effect with lower daily  $\text{NO}_x$  and higher MDA8  $\text{O}_3$  on Sundays compared to Wednesdays, an indication of  $\text{NO}_x$  saturation.<sup>56</sup> Wolff et al.<sup>57</sup> observed urban areas across the United States trending away from the weekend effect over time, with the Chicago area weekend MDA8 10+ % greater than weekday in 1997–1999 tapering down to ~5–10% higher in 2008–2010. Sensitivity simulations based on 2005 emissions by Koo et al.<sup>31</sup> showed that weekend reductions in  $\text{NO}_x$  emissions in the Chicago area resulted in  $\text{O}_3$  increases locally and immediately downwind, but  $\text{O}_3$  decreased farther downwind. First-order DDM weekend  $\text{NO}_x$  sensitivities were negative in the urban center ( $\text{NO}_x$ -saturated) and positive outside the urban center ( $\text{NO}_x$ -limited).

Figure 5 (bottom panels) shows the Chicago area MDA8 sensitivity in 2007 (left) and 2016 (right) based on the response to a 20% anthropogenic  $\text{NO}_x$  cut for May–September days with modeled MDA8 greater than 70 ppb. The relatively large zone of  $\text{NO}_x$  saturation (yellow) in 2007 generally covers the urban and industrial centers. The spatial extent of  $\text{NO}_x$  saturation decreased in size by 2016. As mentioned previously, Figure 1 shows a DOW boxplot analysis for the area. The monitoring data show lower  $\text{O}_3$  on weekends compared to weekdays for both 2007 (not significant) and 2016 (significant) when averaging all May–September MDA8 across the 16 monitoring locations with complete data which were in operation in both years in the Chicago nonattainment area. This includes both the urban core (relatively higher precursor emissions and lower  $\text{O}_3$ ) and downwind (relatively lower precursor emissions and higher  $\text{O}_3$ ) sites. The corresponding model results show statistically significant modeled mean differences of 2.6 ppb in 2007 and −1.9 ppb in 2016, indicating a transition in chemical sensitivity from  $\text{NO}_x$ -saturated to  $\text{NO}_x$ -limited when analyzing the area as a whole. Substantial  $\text{NO}_x$  emission reductions have occurred during this time period (Table S1 listed by state and nationwide total). For the counties in the Chicago tri-state nonattainment area, specifically, the  $\text{NO}_x$  reductions were ~44%, going from modeled emissions of roughly 360 K tons

per year (tpy) in 2007 to 202 K tpy in 2016. Similarly, de Foy<sup>58</sup> observed a 50% decrease in measured  $\text{NO}_x$  concentrations from 2005 to 2016 when looking at 6 monitors in the Chicago area, with the average weekend  $\text{NO}_x$  reductions stronger in more commercial areas ( $\sim 45\%$   $\text{NO}_x$  reduction on Sundays) than residential areas ( $\sim 30\%$   $\text{NO}_x$  reduction on Sundays).

While the area-wide mean weekend differences for 2016 presented here are statistically significant, none of the mean differences at the individual monitoring locations are statistically significant, likely owing to the small sample size for one monitor for 1 year (May–September). However, the comparison at individual monitors (see locations in Figure 7) is useful for gleaning more specific DOW information for

in 2020. At Kenosha (AQS ID: 550590019), the median weekday  $\text{O}_3$  was roughly the same in 2016 as 2007, but both the weekday 75th percentile and the overall weekend  $\text{O}_3$  decreased by 2016 (Figure S10). At Northbrook (170314201), median weekday  $\text{O}_3$  increased in 2016 compared to 2007, but the weekday 75th percentile and the overall weekend  $\text{O}_3$  decreased (Figure S5). The data comparison between 2007 and 2016 suggests that both the Kenosha and Northbrook sites may have switched from  $\text{NO}_x$ -saturated to  $\text{NO}_x$ -limited; Kenosha switched from a positive mean weekend difference to a negative mean weekend difference, 0.02 to  $-3.9$  ppb (modeled 2.5 to  $-2.5$  ppb), and the Northbrook mean weekend difference became more negative,  $-0.5$  to  $-3.1$  ppb, and switched from positive to negative in the modeled data, 3.4 to  $-2.6$  ppb. Likewise, the  $\text{O}_3$  isopleths for Northbrook (Figure 8) and Kenosha (Figure S32) each show a clear transition from  $\text{NO}_x$  saturation to  $\text{NO}_x$ -limitation going from 2007 to 2016.

The  $\text{O}_3$  isopleths demonstrate how the changes in the chemical regime at Kenosha and Northbrook have impacted model predictions for control strategies. At both monitors, the 2007  $\text{O}_3$  isopleths do not show a clear path for attaining the  $\text{O}_3$  standard using  $\text{NO}_x$  emission reductions alone, although the  $\text{O}_3$  isopleths are not expected to provide accurate  $\text{O}_3$  predictions for  $\text{NO}_x$  emission changes larger than approximately 50%. The 2016  $\text{O}_3$  isopleths, which represent conditions with much lower  $\text{NO}_x$  emissions, indicate  $\text{NO}_x$  reductions in the range of 50% could bring average  $\text{O}_3$  at the Kenosha and Northbrook monitors below 71 ppb on high  $\text{O}_3$  days. These  $\text{O}_3$  isopleths provide information about average  $\text{O}_3$  response on modeled days with high  $\text{O}_3$  but do not specifically show how the regulatory metric (the design value or 4th highest MDA8 averaged over 3 years) would respond to emission reductions. At both sites, the 2016  $\text{O}_3$  isopleths suggest that anthropogenic VOC emission reductions would reduce the total  $\text{NO}_x$  reductions needed to bring  $\text{O}_3$  levels down. As mentioned previously, these isopleths make no assumptions about where  $\text{O}_3$  is produced. Since the  $\text{O}_3$  isopleths are derived from the HDDM applied at a national scale, the changes in any location incorporate the impact of both local production and  $\text{O}_3$  transport. Therefore, while not shown specifically in the  $\text{O}_3$  isopleths, precursor emission reduction upwind is also expected to benefit these downwind sites.

Sites upwind of Kenosha and Northbrook include, but are not limited to, the monitor just southeast of the O'Hare International Airport (170311003), the Cicero IL monitor (170314002), and the Lemont, IL, monitor (170311601), none of which had design values above the NAAQS in 2016 (Table 1). Each of these sites (located on the map in Figure 7) showed a trend toward  $\text{NO}_x$ -limitation (i.e., a relative shift toward more negative differences) going from 2007 to 2016 in both monitoring and modeled data as well as the associated  $\text{O}_3$  isopleths (see Figures S5–S12 and S29–S33), although the trends were not as pronounced as those for the two downwind monitors mentioned above. Additionally, as  $\text{NO}_x$  emissions decreased, the model predicted more high  $\text{O}_3$  days ( $>71$  ppb MDA8) at each of these sites in 2016 than 2007. The site near O'Hare is  $\sim 15$  miles west and slightly north of downtown Chicago. The DOW boxplot for this site showed a slightly greater median weekday and roughly the same median weekend  $\text{O}_3$  in 2016 compared to 2007, but the 75th percentile for both weekdays and weekends and the 95th

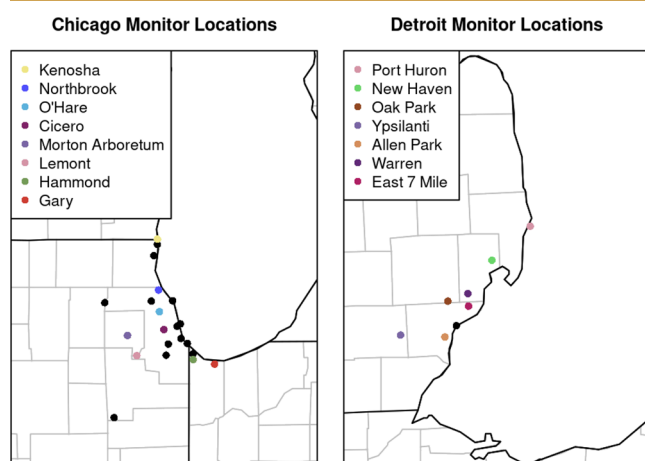


Figure 7. Locations of Chicago and Detroit  $\text{O}_3$  monitoring sites.

various parts of the area, which is a relatively large nonattainment area with varying spatial distribution of precursor emission sources. Two downwind monitoring sites with the measured design values above the standard in 2016 (Table 1) include the Kenosha WI (77 ppb) and Northbrook IL (71 ppb) sites located 50 and 20 miles north of downtown Chicago, respectively. Both sites were also above the standard

Table 1. Design Values (DV)<sup>a</sup> at Chicago and Detroit  $\text{O}_3$  Monitoring Sites

Chicago			Detroit		
monitor location	2016 DV (ppb)	2020 DV (ppb)	monitor location	2016 DV (ppb)	2020 DV (ppb)
Kenosha	77	74	Port Huron	73	71
Northbrook	71	77	New Haven	72	71
O'Hare	69	73	Warren	67	68
Cicero	66	71	East 7 Mile	72	71
Morton Arboretum	68	71	Oak Park	69	72
Lemont	69	71	Ypsilanti	67	67
Hammond	65	66	Allen Park	65	67
Gary	67	70			

<sup>a</sup>Design values are the 3 year average of the 4th highest MDA8 at each site, the regulatory metric for determining whether the site is meeting the  $\text{O}_3$  standard. The 2015  $\text{O}_3$  NAAQS (or  $\text{O}_3$  standard) is set at 70 ppb in the United States.

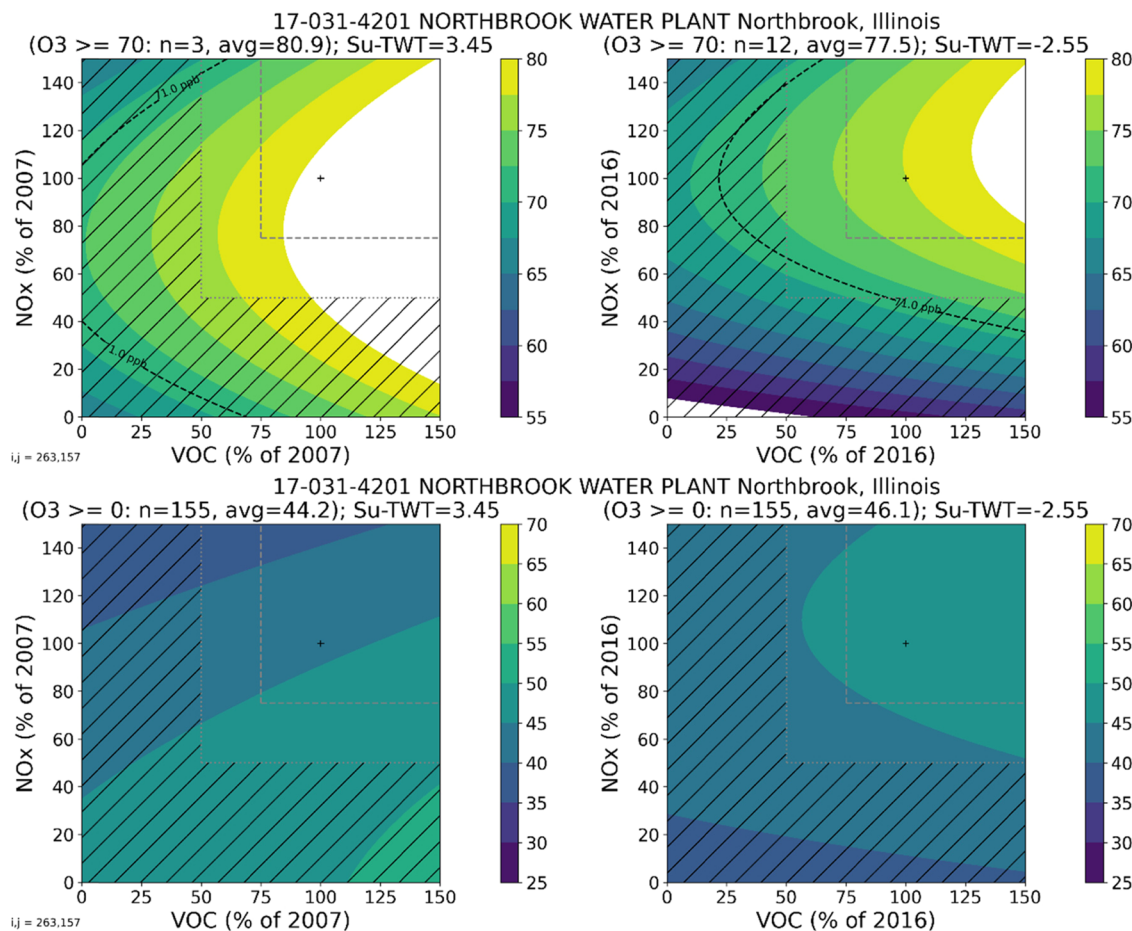


**Figure 8.**  $O_3$  isopleths in 2007 (left) and 2016 (right) for all MDA8 ( $O_3 > 0$ ) (bottom panels) and high MDA8 ( $O_3 > 70$  ppb) (top panels) for the Northbrook, IL, monitor in the Chicago nonattainment area. Color bars indicate the corresponding  $O_3$  isopleth value. Dashed boxes are shown at 50 and 75% of original emissions, and hatching covers the area where large emission reductions (from 50–100%) are outside the domain of the expected HDDM accuracy. The curved dotted line depicts locations in the  $O_3$  isopleth space that match 71 ppb MDA8  $O_3$ , below which the site would not be modeling exceedances of the 2015  $O_3$  NAAQS.

percentile weekend  $O_3$  decreased by 2016 (Figure S7). Figure S29 shows O'Hare with a transitional regime on high  $O_3$  days in both 2007 and 2016. The Cicero site is ~8 miles southwest of downtown Chicago, just north of the Chicago Midway International Airport, located in the vicinity of several rail intermodal facilities, and surrounded by many industrial point sources. While MDA8  $O_3$  was often below 60 ppb at Cicero in both years,  $O_3$  generally increased from 2007 to 2016 at this site, with only the 75th and 95th percentile weekend  $O_3$  decreasing (Figure S8). Accordingly, the  $O_3$  isopleths show the chemical regime at this site moving from  $NO_x$ -saturated to transitional as  $NO_x$  emissions decreased (Figure S30). The Lemont, IL, monitoring site is ~24 miles southwest of downtown Chicago, just south of the Argonne National Laboratory and the Des Plaines River, near several county forest preserves, and surrounded by several highways and many industrial point sources, which are predominately located along the river.  $O_3$  decreased from 2007 to 2016 at this site (Figure S9) and moved from a transitional chemical regime in 2007 to a  $NO_x$ -limited regime in 2016 on high  $O_3$  days (Figure S31).

Two additional upwind locations, the Hammond (180892008) and Gary (180890022) monitors both located in Lake County in northwest IN roughly 20 miles southeast of downtown Chicago, near the Gary/Chicago International airport, and in the vicinity of several major interstate roadways,

railways, railyards, and industrial point sources showed lower  $O_3$  on weekends (not significant) with a weaker mean difference going from 2007 to 2016. The measured mean difference went from -1.4 to -0.9 ppb for Hammond (Figure S11) and -3.8 to -1.7 for Gary (Figure S6). While this would tend to indicate  $O_3$  sensitivity becoming relatively less  $NO_x$ -limiting for this portion of the nonattainment area based on the weekend effect, the  $O_3$  isopleths for Hammond and Gary show movement from  $NO_x$  saturation toward  $NO_x$ -limitation (or transitional for days with modeled MDA8 > 70 ppb, see Figure 9 for Gary and Figure S33 for Hammond). As mentioned previously, the DOW analysis (measured or modeled) does not account for meteorological differences in weekends versus weekdays which may vary between years. The specific meteorology for these shoreline sites in 2007 and 2016 may have played a role in the DOW differences between years. In contrast, the HDDM analysis looks strictly at chemistry feedback in the model and is not constrained by DOW meteorological patterns. The change in HDDM-based  $O_3$  sensitivity was likely driven by the large decreases in modeled  $NO_x$  emissions for Lake County, IN, going from approximately 44,000 tpy (2007) to 24,000 tpy (2016), with decreases from point and onroad sources accounting for most of this change. While measured  $O_3$  generally decreased from 2007 to 2016 at these sites, weekend values at the low end of the distribution

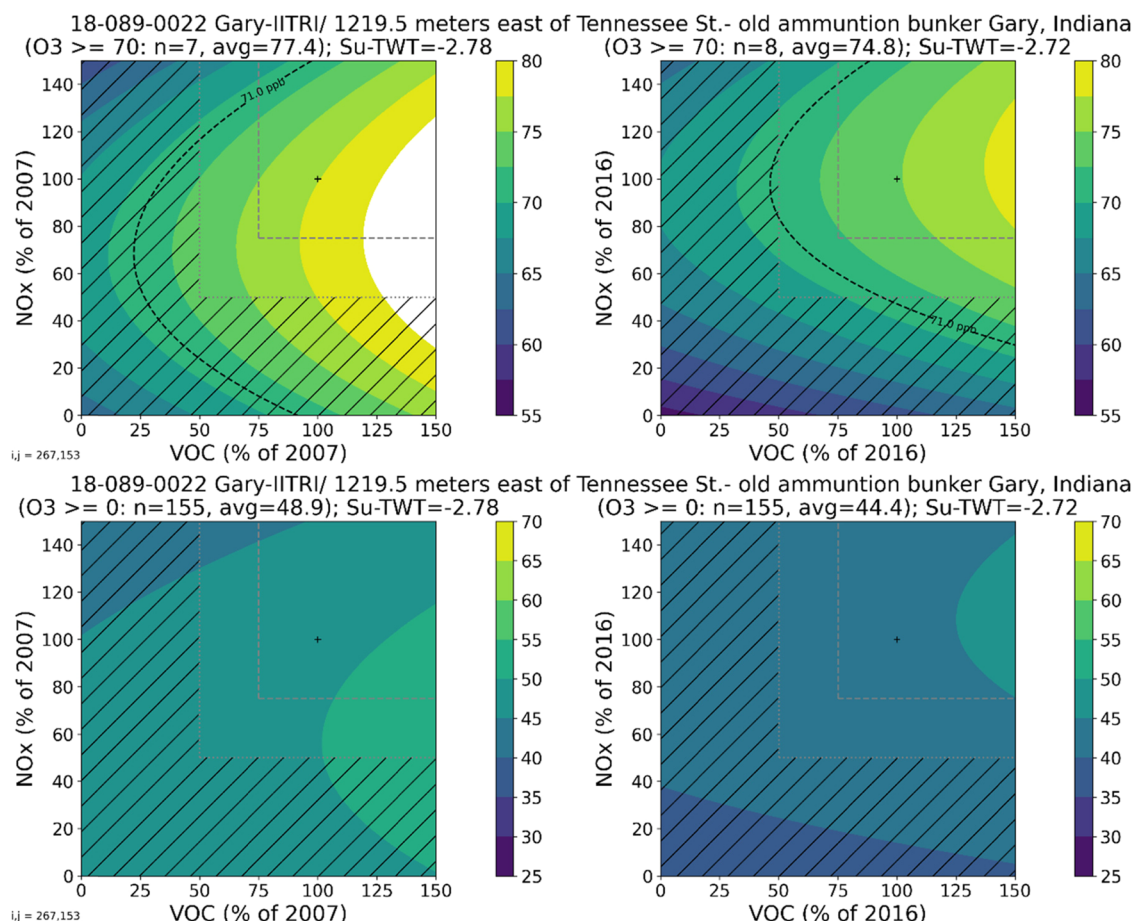


Figure 9. The same as Figure 8 for the Gary, IN, monitor in the Chicago nonattainment area.

(bottom whiskers in Figures S5 and S6) increased at both sites from 2007 to 2016 (more pronounced for Gary than Hammond). This pattern suggests that the previously mentioned  $\text{NO}_x$  reductions in this area may have resulted in less titration during the transition away from  $\text{NO}_x$  saturation. However, because of the limited number of weekend days in this analysis, it is difficult to draw definitive conclusions about behavior at the extreme ends of the observed  $\text{O}_3$  distributions.

The DOW analysis using observations shows only one site in the entire Chicago area (170436001 near the Morton Arboretum in DuPage County, Figure S12) with higher median (no Chicago area sites have higher 95th percentile  $\text{O}_3$  values on weekends than weekdays in 2016)  $\text{O}_3$  on weekends than weekdays in 2016 (indicative of lingering local  $\text{NO}_x$  saturation). Similarly, the model predicts that the zone of  $\text{NO}_x$  saturation in Chicago decreased substantially from 2007 to 2016, although there are some small portions of the area still exhibiting modeled  $\text{NO}_x$  saturation (Figure 5). As mentioned previously,  $\text{NO}_x$ -saturated conditions dampen the responsiveness of local  $\text{O}_3$  formation to local  $\text{NO}_x$  emission controls in the near term, presenting complex scenarios for air quality managers. Further investigations into  $\text{O}_3$  sensitivity across the Chicago area and the impacts downwind may be helpful in verifying these results and informing ongoing air quality management efforts and emission control strategy development at local and regional scales.

**3.3.2. Detroit.** The Detroit Michigan area shares an international border with the Ontario Province of Canada, following from north to south Lake Huron, the St. Clair River,

Lake St. Clair, the Detroit River, and Lake Erie. The Michigan–Ontario airshed experiences high  $\text{O}_3$  episodes that are influenced by high precursor emissions and local and synoptic meteorology. Recent back-trajectories from the Detroit area  $\text{O}_3$  monitors show air flow predominately from the west, southwest, and southerly directions on high  $\text{O}_3$  days.<sup>55</sup> The results of the 2007 Border Air Quality and Meteorology Study (BAQS-Met) in southwestern Ontario indicate that the nearby lakes influence local meteorology such that local anthropogenic emissions have an impact closer to populated source areas than would otherwise occur in the absence of the lakes. This includes shallow inversions above the cool lake water, which confine pollutants in a relatively small volume, and recirculation of pollutants in both the vertical (weaker synoptic flow) and horizontal (stronger synoptic flow) dimensions. The spatial extent of the boundary-layer features associated with these processes can be small with narrow elongated lines along frontal convergence zones, likewise, resulting in spatial heterogeneity of  $\text{O}_3$  impact.<sup>59</sup> For instance, local  $\text{O}_3$  peaks were observed  $\sim 30$  ppb above the regional background. Such localized  $\text{O}_3$  enhancements may only be detected by a small number of monitors or go undetected.<sup>59</sup> Model sensitivity analyses suggest that instantaneous  $\text{O}_3$  formation in southwestern Ontario was VOC-limited in 2007,<sup>60</sup> but MDA8 showed  $\text{NO}_x$ -sensitivity based on Sillman indicators.<sup>59</sup>

Several studies have observed changes in the Detroit area  $\text{O}_3$  regime over time. Jin et al.<sup>8</sup> conducted a study of various areas using GEOS-Chem modeling, OMI satellite data retrievals, and

formaldehyde to  $\text{NO}_x$  ratios, finding the Detroit area trending toward  $\text{NO}_x$ -limitation going from 2005 to 2015. Wolff et al.<sup>57</sup> observed urban areas across the United States trending away from the weekend effect over time, with Detroit area weekend MDA8 ranging from 5 to 10+ % greater than weekdays in 1997–1999 and tapering down to the range of 5% higher to 5% lower compared to weekdays in 2008–2010 at several monitoring sites.

Pierce et al.<sup>30</sup> observed and modeled a less pronounced weekend effect at Detroit area monitoring locations when going from 1988–1993 to 2000–2005. The Pierce et al.<sup>30</sup> CMAQ modeling also indicated a general transition away from  $\text{NO}_x$  saturation toward  $\text{NO}_x$ -limitation when comparing the ratio of modeled  $\text{O}_3$  to modeled  $\text{NO}_z$  ( $\text{NO}_y - \text{NO}_x$ ) for these same two sets of time periods in the Detroit area.

Figure 5 (the second row from the bottom) shows the Detroit area  $\text{O}_3$  sensitivity in 2007 (left) and 2016 (right) based on the response to a 20% cut in anthropogenic  $\text{NO}_x$  for May–September with modeled MDA8 greater than 70 ppb. The zone of  $\text{NO}_x$  saturation (yellow) in 2007 includes a portion of the area generally covering urban and industrial centers nearest the lake, whereas the rest of the area is generally  $\text{NO}_x$ -limited (blue). This is consistent with the Koo et al.<sup>31</sup> CAMx simulation for 2005, in which the Detroit urban center was  $\text{NO}_x$ -saturated and the surrounding areas showed  $\text{NO}_x$ -sensitivity. In the present study, the geographic zone (spatial extent) of  $\text{NO}_x$  saturation disappeared completely by 2016. Figure 10 shows a DOW boxplot analysis for the Detroit

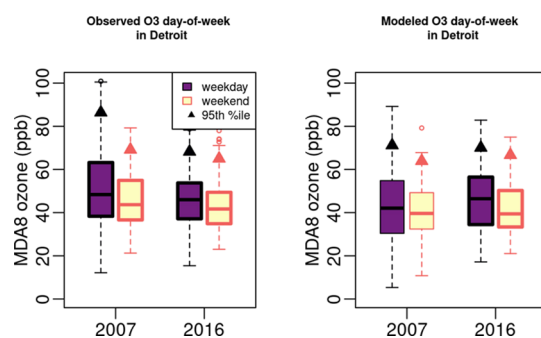


**Figure 10.** May–September weekday versus weekend MDA8  $\text{O}_3$  in the Detroit nonattainment area for 2007 and 2016 based on monitored values (left panel) and modeled values in grid cells containing monitor locations (left panel). Boxes represent the 25th–75th percentile, horizontal lines represent median values, whiskers extend to 1.5× the interquartile range, dots show outlier values, and triangles represent 95th percentile values. A bold outline around a box indicates a significant difference ( $p < 0.05$ ).

area. The monitoring data show lower  $\text{O}_3$  on weekends with a mean difference of  $-5.8$  and  $-3.2$  ppb (both statistically significant;  $p$ -value  $<0.01$ ) compared to weekdays for 2007 and 2016, respectively, when averaging May–September MDA8 across the monitoring locations with complete data which were in operation in both years in the current Detroit nonattainment area. The corresponding model results show a mean difference of  $-1.3$  ppb in 2007 (not statistically significant;  $p$ -value = 0.31) and  $-3.7$  ppb in 2016 (statistically significant  $p$ -value  $<0.01$ ), indicating that the area has generally been  $\text{NO}_x$ -limited over time. The modeled and observed weekend effects are both about  $-3$  ppb in 2016; however, the model suggests a stronger weekend effect in 2016 relative to 2007, whereas the observations suggest a weaker effect (increasing to  $-3.2$  ppb in

2016 from  $-5.8$  ppb in 2007). This example highlights both the potentially confounding influence of year-to-year meteorological variability in this type of analysis, as well as the challenges in resolving air pollution chemistry using photochemical models in complex urban areas with evolving local emissions.

A comparison at individual monitors (Figure 7 and Table 1) shows New Haven (260990009) and Port Huron (261470005), the northeastern-most monitoring sites and generally the farthest downwind, both had measured  $\text{O}_3$  design values above 70 ppb in 2016. These sites had lower measured  $\text{O}_3$  on weekends, indicating  $\text{NO}_x$ -limitation in both years:  $-8.4$  and  $-8.1$  ppb, respectively, (both significant) in 2007 and  $-4.1$  and  $-4.7$  ppb, respectively, (neither significant) in 2016 (Figures S13 and S14). Likewise, the modeled differences show lower  $\text{O}_3$  on the weekends (not significant) for both sites for both years. The  $\text{O}_3$  isopleths (Figures S34 and S35) generally show  $\text{NO}_x$ -limitation for both sites for both years, particularly for days with MDA8 above 70 ppb. The New Haven and Port Huron sites would have needed greater than a 50% reduction in  $\text{NO}_x$  from 2007 modeled emission levels to avoid high  $\text{O}_3$  days, but uncertainty in HDM projections beyond 50% prevent us from quantifying how much greater. Anthropogenic  $\text{NO}_x$  and VOC emissions in Michigan declined by approximately 46 and 26%, respectively, between the 2007 and 2016 modeling simulations (Table S1). Both sites would need a roughly 20%  $\text{NO}_x$  reduction from 2016 levels on high  $\text{O}_3$  days to obtain below 71 ppb MDA8 based on the  $\text{O}_3$  isopleths. Unlike the Chicago sites, discussed in Section 3.3.1, the  $\text{O}_3$  isopleths presented here indicate that anthropogenic VOC emission reductions would have little impact on  $\text{O}_3$  concentrations for these days and would not substantially impact the  $\text{NO}_x$  reductions needed for these sites.

Slightly upwind from New Haven and Port Huron is a cluster of three monitors, including Warren (260991003), East 7 Mile (261630019), and Oak Park (261250001). Among these, only the East 7 Mile site had a design value above the 70 ppb  $\text{O}_3$  standard in 2016, although the Oak Park monitor has the highest design value for 2020 at 72 ppb (Table 1). While none of the weekend differences were significant, each of these monitors measured lower  $\text{O}_3$  on weekends than weekdays by  $\sim 6$  ppb in 2007 and  $\sim 4$  ppb in 2016 (Figures S15–S17). The modeled differences for 2007 were 1.0 ppb higher, 1.3 ppb higher, and 0.5 ppb lower on weekends for Warren, East 7 Mile, and Oak Park, respectively, and 3–4 ppb lower on weekends in 2016. The  $\text{O}_3$  isopleths (Figures S36–S38) indicate that these three sites were generally  $\text{NO}_x$ -saturated in 2007 and flipped to  $\text{NO}_x$ -limited by 2016. The 2016  $\text{O}_3$  isopleths indicate a roughly 35%  $\text{NO}_x$  cut would be needed on high  $\text{O}_3$  days for the East 7 Mile site to stay below 71 ppb MDA8 (Figure S37). Similar to the New Haven and Port Huron sites, the 2016  $\text{O}_3$  isopleths for the East 7 Mile monitor indicate anthropogenic VOC emission reductions having little impact on  $\text{O}_3$  levels on high days. The  $\text{O}_3$  isopleths for a fourth site, the Allen Park monitor (261630001) (boxplot in Figure S18), which is roughly 16 miles upwind of this cluster of three monitors, showed a switch from transitional chemistry in 2007 to  $\text{NO}_x$ -limited conditions in 2016 (Figure S39). A fifth site, the Ypsilanti monitor (261610008), which is farther upwind (roughly 30 miles from the clump of three monitors) also had lower measured and modeled  $\text{O}_3$  on weekends compared to weekdays (not significant) in both years (Figure S19). The

Ypsilanti O<sub>3</sub> isopleths show a tendency toward NO<sub>x</sub> saturation (all days) and NO<sub>x</sub>-limitation (high days) (Figure S40).

While the average behavior on high O<sub>3</sub> days indicates NO<sub>x</sub>-limitation, there may be individual days that remain NO<sub>x</sub>-saturated. For example, at the Ypsilanti monitor, the model predicted 9 days in 2007 and 3 days in 2016 with MDA8 greater than 70 ppb (Table S3). When applying the 2016 estimated emission reductions (45% in NO<sub>x</sub> and 25% in VOC) to the 2007 O<sub>3</sub> isopleths, 3 of those 9 days are predicted to drop below 70 ppb MDA8. In addition, there were 2 days that did not exceed 70 ppb MDA8 in 2007 but are projected to in 2016, one of which was in the original 9 days (70 to 71.7 ppb) and the other increased from 69 to 74.9 ppb (not shown). Overall, for days exceeding 70 ppb MDA8, the O<sub>3</sub> isopleths predicted that the 2007 average for those 9 days would drop from 75.3 to ~71 ppb. The top 9 days in the 2016 modeling (with different meteorology) had an average MDA8 of 66.5 ppb. Despite several NO<sub>x</sub>-saturated days, the high-end of the distribution still decreased as predicted by the average O<sub>3</sub> isopleths for days greater than 70 ppb MDA8.

Further investigations into O<sub>3</sub> sensitivity in the various portions of this airshed during various high O<sub>3</sub> episodes may inform ongoing air quality management efforts and emission control strategy development at a more local scale. This area could also benefit from finer-scale modeling and intensive measurements to analyze O<sub>3</sub>, precursors, and meteorology.

### 3.4. Limitations and Uncertainties

While the modeling results in this work generally agreed with available observations and previous analyses, there are several limitations to our approach. First, our conclusions about changes and trends in O<sub>3</sub> production chemistry are based on a comparison of two specific years, 2016 and 2007. O<sub>3</sub> formation is very sensitive to meteorological factors that can vary greatly from year to year; a more robust comparison would therefore involve examining groupings of multiple years or a continuous time series, as well as additional analysis to explicitly isolate relative contributions of meteorology and emissions to O<sub>3</sub> variations. Such an analysis using photochemical modeling instrumented with the HDDM was computationally prohibitive for this assessment but would be of interest for future work. We did examine WE–WD differences in temperature at meteorological stations colocated with the AQS monitors for 2007 and 2016 (Figure S42) and found that eight areas experienced statistically significant WE–WD temperature differentials during one or both years. Given the understanding that higher temperatures are often associated with higher O<sub>3</sub> concentrations,<sup>61</sup> the WE–WD temperature results cannot explain the WE–WD results observed for O<sub>3</sub> in the areas examined. Several areas experienced a correlation between higher temperatures and higher O<sub>3</sub> on either WE or WD, but in these cases, the WE–WD differentials for O<sub>3</sub> were highly significant (i.e., *p*-values less than 0.01), suggesting that the observed WE–WD O<sub>3</sub> patterns would also hold under different temperature conditions. The exception was Denver, an area where the correspondence of DOW patterns to emission-driven O<sub>3</sub> variations is inherently complicated by the potential influence of stratospheric intrusions, as shown in a previous study.<sup>62</sup>

The CAMx results presented in this analysis may be biased for individual locations because of undiagnosed errors in emissions, chemistry, or meteorology. Similarly, while our modeling appears to have qualitatively captured the trend

toward NO<sub>x</sub>-limitation happening in most areas of the country, it is not clear from our analysis how precisely the model captures the timing of these transitions, for example, the model may have already shown transitions toward NO<sub>x</sub>-limited conditions in years prior to 2016 that were not present in the observations, or vice versa. Also, despite capturing the overall trend toward more NO<sub>x</sub>-limited conditions, the magnitude of the model's response to the WE–WD emission changes does not always match the observed magnitude, both within and across individual years. Finally, as mentioned above, it is likely that CAMx and other regional air quality modeling tools at ~12 km spatial resolution may not fully capture hyper-local features in emissions and/or meteorology that govern O<sub>3</sub> formation in complex urban areas, including those located along land-water interfaces.

Continuing to evaluate and monitor the responsiveness of O<sub>3</sub> formation to precursor emission changes across the United States will be an ongoing need for air quality managers moving forward as emission distributions continue to evolve. Given the limitations mentioned above, other modeling techniques and analysis tools will continue to be an informative complement to air quality modeling-based assessments. For example, Jin et al.<sup>7</sup> combined long-term observations from satellites with surface measurements to characterize trends in summertime O<sub>3</sub> chemistry over the United States, demonstrating the potential utility of space-based approaches for understanding local-scale O<sub>3</sub> chemistry relevant for air quality. These limitations also highlight a need to improve our ability to characterize fine-scale environments with regional-scale models. New data from recent field campaigns such as the Long Island Sound Tropospheric Ozone Study (LISTOS), the Lake Michigan Ozone Study (LMOS), and the Michigan–Ontario Ozone Source Experiment (MOOSE) offer exciting opportunities to rigorously evaluate our suite of existing modeling tools in complicated urban environments. For instance, Vermeuel et al.<sup>63</sup> were able to develop observationally based indicators to characterize complex urban plume dynamics and influence on local O<sub>3</sub> production chemistry across the Chicago area based on data from the LMOS campaign.

## 4. CONCLUSIONS

In this work, we used ground monitoring data and high-resolution regional air quality modeling to characterize the state of O<sub>3</sub> production chemistry across the United States. Our goals were twofold: (1) assess how well modeling tools used for policy and regulatory assessments compare to ambient observations and similar analyses from the broader scientific community, and (2) better understand the state of O<sub>3</sub> production chemistry in different regions of the country that experience a range of emission sources and meteorological conditions. The DOW analysis using ambient and modeled O<sub>3</sub> values produced broadly consistent results within and between individual years. The one location where conclusions derived from our modeling results showed fundamental discrepancies with the observations was Los Angeles/Southern California, a complex metropolitan area that could likely be better resolved at finer spatial resolutions than the 12 km domain applied here. At a national scale, both our DOW and HDDM analyses show trends toward NO<sub>x</sub>-limited conditions across most of the United States, although some areas remain complex (i.e., exhibit transitional behavior, specifically a handful of urban areas in California and the Upper Midwest).

This broad pattern toward  $\text{NO}_x$ -limitation is consistent with previous studies.<sup>7,8,64</sup> The general agreement with surface monitor observations through DOW analysis provides support for the continued use of existing air quality modeling tools for such assessments. Our assessments of Chicago and Detroit also highlight the spatial variability in  $\text{O}_3$  chemistry that can occur within a particular urban area, emphasizing the need for continued development of tools and approaches for characterizing  $\text{O}_3$  responsiveness to emission reductions at local scales.

The model maps show that  $\text{NO}_x$  saturation still occurs in select urban cores. However, the areas surrounding these  $\text{NO}_x$ -saturated spots are  $\text{NO}_x$ -limited and are affected by upwind urban  $\text{NO}_x$  emissions. This highlights the continued need for  $\text{NO}_x$  reductions. As  $\text{NO}_x$  is reduced, even the  $\text{NO}_x$ -saturated areas will become more  $\text{NO}_x$ -limited. In the short term, VOC reduction strategies may be paired with  $\text{NO}_x$  reductions to ensure  $\text{O}_3$  mitigation in urban cores as well as the surrounding areas. The Houston area highlights the potential successes associated with targeted VOC reductions. The 2007 period showed  $\text{NO}_x$  saturation around the ship channel in both the DOW and HDDM analyses, but by 2016 has transitioned to  $\text{NO}_x$ -limitation only. Over that same period, both VOC and  $\text{NO}_x$  controls were put in place to separately address localized highly reactive VOC releases and the broader  $\text{NO}_x$  problem.<sup>65,66</sup>

Our results support previous findings that most of the United States is transitioning or has already transitioned to  $\text{NO}_x$ -limited chemistry during the summertime high  $\text{O}_3$  season, supporting the need for continued  $\text{NO}_x$  emission reductions to further mitigate  $\text{O}_3$  pollution. However, it is important to note that many VOC compounds are classified as hazardous air pollutants.<sup>67</sup> Some VOCs are also precursors for secondary particulate matter formation.<sup>68</sup> Emission controls for these VOC compounds would consequently be beneficial for public health beyond their impact on  $\text{O}_3$ . For this study, we define  $\text{NO}_x$ -limited conditions as those for which  $\text{NO}_x$  emission reductions are more effective at reducing  $\text{O}_3$  than VOC emission reductions; however, anthropogenic VOC reductions may still reduce  $\text{O}_3$  for these areas. Further reductions in VOC concentrations for the purposes of minimizing public exposure to air toxics and particulates may therefore result in  $\text{O}_3$  cobenefits despite prevailing  $\text{NO}_x$ -limitation.

## ■ ASSOCIATED CONTENT

### Supporting Information

The Supporting Information is available free of charge at <https://pubs.acs.org/doi/10.1021/acsenvironau.1c00029>.

Tables detailing anthropogenic emissions used in CAMx HDDM modeling and chemical regime determinations from the DOW analysis; Monte Carlo testing for DOW results in select cities; additional DOW barplots and  $\text{O}_3$  isopleth diagrams for individual monitors in Chicago and Detroit; additional chemical sensitivity maps by region; DOW  $\text{O}_3$  differentials plotted against HDDM-calculated  $\text{O}_3$  changes; and nonattainment area DOW temperature differentials (PDF)

## ■ AUTHOR INFORMATION

### Corresponding Author

**Shannon Koplitz** — *Office of Air Quality Planning and Standards, U.S. Environmental Protection Agency, Research Triangle Park, North Carolina 27711, United States;*

*Triangle Park, North Carolina 27711, United States;*

 [orcid.org/0000-0003-1745-903X](https://orcid.org/0000-0003-1745-903X);

Email: [koplitz.shannon@epa.gov](mailto:koplitz.shannon@epa.gov)

## Authors

**Heather Simon** — *Office of Air Quality Planning and Standards, U.S. Environmental Protection Agency, Research Triangle Park, North Carolina 27711, United States;*

 [orcid.org/0000-0001-7254-3360](https://orcid.org/0000-0001-7254-3360)

**Barron Henderson** — *Office of Air Quality Planning and Standards, U.S. Environmental Protection Agency, Research Triangle Park, North Carolina 27711, United States*

**Jennifer Liljegren** — *Region 5, U.S. Environmental Protection Agency, Research Triangle Park, North Carolina 27711, United States*

**Gail Tonnesen** — *Region 8, U.S. Environmental Protection Agency, Research Triangle Park, North Carolina 27711, United States*

**Andrew Whitehill** — *Office of Research and Development, U.S. Environmental Protection Agency, Research Triangle Park, North Carolina 27711, United States*

**Benjamin Wells** — *Office of Air Quality Planning and Standards, U.S. Environmental Protection Agency, Research Triangle Park, North Carolina 27711, United States*

Complete contact information is available at:

<https://pubs.acs.org/10.1021/acsenvironau.1c00029>

## Notes

The views expressed in this manuscript are those of the authors alone and do not necessarily reflect the views and policies of the U.S. Environmental Protection Agency.

The authors declare no competing financial interest.

## ■ ACKNOWLEDGMENTS

The authors thank Lukas Valin (EPA/ORD) for his thoughtful insights and suggestion to explore DOW analysis for this work. We also thank Kristin Foley (EPA/ORD) and Christian Hogrefe (EPA/ORD) for their helpful comments during internal review.

## ■ REFERENCES

- (1) Kleinman, L. I.; Daum, P. H.; Lee, Y. N.; Nunnermacker, L. J.; Springston, S. R.; Weinstein-Lloyd, J.; Rudolph, J. A comparative study of ozone production in five U.S. metropolitan areas. *J. Geophys. Res.: Atmos.* **2005**, *110*, D02301.
- (2) Sillman, S.; Logan, J. A.; Wofsy, S. C. The sensitivity of ozone to nitrogen oxides and hydrocarbons in regional ozone episodes. *J. Geophys. Res.: Atmos.* **1990**, *95*, 1837–1851.
- (3) Simon, H.; Reff, A.; Wells, B.; Xing, J.; Frank, N. Ozone trends across the United States over a period of decreasing NO<sub>x</sub> and VOC emissions. *Environ. Sci. Technol.* **2015**, *49*, 186–195.
- (4) Xing, J.; Pleim, J.; Mathur, R.; Pouliot, G.; Hogrefe, C.; Gan, C.-M.; Wei, C. Historical gaseous and primary aerosol emissions in the United States from 1990 to 2010. *Atmos. Chem. Phys.* **2013**, *13*, 7531–7549.
- (5) McDonald, B. C.; de Gouw, J. A.; Gilman, J. B.; Jathar, S. H.; Akherati, A.; Cappa, C. D.; Jimenez, J. L.; Lee-Taylor, J.; Hayes, P. L.; McKeen, S. A.; Cui, Y. Y.; Kim, S. W.; Gentner, D. R.; Isaacman-VanWertz, G.; Goldstein, A. H.; Harley, R. A.; Frost, G. J.; Roberts, J. M.; Ryerson, T. B.; Trainer, M. Volatile chemical products emerging as largest petrochemical source of urban organic emissions. *Science* **2018**, *359*, 760–764.
- (6) Guenther, A.; Hewitt, C. N.; Erickson, D.; Fall, R.; Geron, C.; Graedel, T.; Harley, P.; Klinger, L.; Lerdau, M.; Mckay, W. A.; Pierce,

T.; Scholes, B.; Steinbrecher, R.; Tallamraju, R.; Taylor, J.; Zimmerman, P. A global model of natural volatile organic compound emissions. *J. Geophys. Res.: Atmos.* **1995**, *100*, 8873–8892.

(7) Jin, X.; Fiore, A.; Boersma, K. F.; Smedt, I. D.; Valin, L. Inferring Changes in Summertime Surface Ozone–NO x–VOC Chemistry over U.S. Urban Areas from Two Decades of Satellite and Ground-Based Observations. *Environ. Sci. Technol.* **2020**, *54*, 6518–6529.

(8) Jin, X.; Fiore, A. M.; Murray, L. T.; Valin, L. C.; Lamsal, L. N.; Duncan, B.; Folkert Boersma, K.; de Smedt, I.; Abad, G. G.; Chance, K.; Tonnesen, G. S. Evaluating a space-based indicator of surface ozone–NOx–VOC sensitivity over midlatitude source regions and application to decadal trends. *J. Geophys. Res.: Atmos.* **2017**, *122*, 10,439–10,461.

(9) Kleinman, L. I.; Lee, Y. N.; Springston, S. R.; Nunnermacker, L.; Zhou, X.; Brown, R.; Hallock, K.; Klotz, P.; Leahy, D.; Lee, J. H.; Newman, L. Ozone formation at a rural site in the southeastern United States. *J. Geophys. Res.: Atmos.* **1994**, *99*, 3469–3482.

(10) Chang, C.-Y.; Faust, E.; Hou, X.; Lee, P.; Kim, H. C.; Hedquist, B. C.; Liao, K.-J. Investigating ambient ozone formation regimes in neighboring cities of shale plays in the Northeast United States using photochemical modeling and satellite retrievals. *Atmos. Environ.* **2016**, *142*, 152–170.

(11) Fiore, A. M.; Jacob, D. J.; Logan, J. A.; Yin, J. H. Long-term trends in ground level ozone over the contiguous United States, 1980–1995. *J. Geophys. Res.: Atmos.* **1998**, *103*, 1471–1480.

(12) Jacob, D. J.; Horowitz, L. W.; Munger, J. W.; Heikes, B. G.; Dickerson, R. R.; Artz, R. S.; Keene, W. C. Seasonal transition from NOx-to hydrocarbon-limited conditions for ozone production over the eastern United States in September. *J. Geophys. Res.: Atmos.* **1995**, *100*, 9315–9324.

(13) Henneman, L. R. F.; Shen, H.; Liu, C.; Hu, Y.; Mulholland, J. A.; Russell, A. G. Responses in ozone and its production efficiency attributable to recent and future emissions changes in the Eastern United States. *Environ. Sci. Technol.* **2017**, *51*, 13797–13805.

(14) Wolff, G. T.; Korsog, P. E. Ozone control strategies based on the ratio of volatile organic compounds to nitrogen oxides. *J. Air Waste Manage. Assoc.* **1992**, *42*, 1173–1177.

(15) Macpherson, A. J.; Simon, H.; Langdon, R.; Misenheimer, D. A mixed integer programming model for National Ambient Air Quality Standards (NAAQS) attainment strategy analysis. *Environ. Model. Softw.* **2017**, *91*, 13–27.

(16) Cardelino, C. A.; Chameides, W. L. An observation-based model for analyzing ozone precursor relationships in the urban atmosphere. *J. Air Waste Manage. Assoc.* **1995**, *45*, 161–180.

(17) Cohen, A. J.; Brauer, M.; Burnett, R.; Anderson, H. R.; Fostad, J.; Estep, K.; Balakrishnan, K.; Brunekreef, B.; Dandona, L.; Dandona, R.; Feigin, V.; Freedman, G.; Hubbell, B.; Jobling, A.; Kan, H.; Knibbs, L.; Liu, Y.; Martin, R.; Morawska, L.; Pope, C. A., III; Shin, H.; Straif, K.; Shaddick, G.; Thomas, M.; van Dingenen, R.; van Donkelaar, A.; Vos, T.; Murray, C. J. L.; Forouzanfar, M. H. Estimates and 25-year trends of the global burden of disease attributable to ambient air pollution: an analysis of data from the Global Burden of Diseases Study 2015. *Lancet* **2017**, *389*, 1907–1918.

(18) Duncan, B. N.; Lamsal, L. N.; Thompson, A. M.; Yoshida, Y.; Lu, Z.; Streets, D. G.; Hurwitz, M. M.; Pickering, K. E. A space-based, high-resolution view of notable changes in urban NOx pollution around the world (2005–2014). *J. Geophys. Res.: Atmos.* **2016**, *121*, 976–996.

(19) Lefohn, A. S.; Malley, C. S.; Smith, L.; Wells, B.; Hazucha, M.; Simon, H.; Paoletti, E. Tropospheric ozone assessment report: Global ozone metrics for climate change, human health, and crop/ecosystem research. *Elementa* **2018**, *6*, 1.

(20) McKeen, S. A.; Hsie, E. Y.; Liu, S. C. A study of the dependence of rural ozone on ozone precursors in the eastern United States. *J. Geophys. Res.: Atmos.* **1991**, *96*, 15377–15394.

(21) Altshuler, S. L.; Arcado, T. D.; Lawson, D. R. Weekday vs. weekend ambient ozone concentrations: discussion and hypotheses with focus on northern California. *J. Air Waste Manage. Assoc.* **1995**, *45*, 967–972.

(22) Blanchard, C. L.; Fairley, D. Spatial mapping of VOC and NOx-limitation of ozone formation in central California. *Atmos. Environ.* **2001**, *35*, 3861–3873.

(23) Brönnimann, S.; Neu, U. Weekend-weekday differences of near-surface ozone concentrations in Switzerland for different meteorological conditions. *Atmos. Environ.* **1997**, *31*, 1127–1135.

(24) Bruntz, S. M.; Cleveland, W. S.; Graedel, T. E.; Kleiner, B.; Warner, J. L. Ozone concentrations in New Jersey and New York: statistical association with related variables. *Science* **1974**, *186*, 257–259.

(25) Cleveland, W. S.; Graedel, T. E.; Kleiner, B.; Warner, J. L. Sunday and workday variations in photochemical air pollutants in New Jersey and New York. *Science* **1974**, *186*, 1037–1038.

(26) de Foy, B.; Brune, W. H.; Schauer, J. J. Changes in ozone photochemical regime in Fresno, California from 1994 to 2018 deduced from changes in the weekend effect. *Environ. Pollut.* **2020**, *263*, No. 114380.

(27) Marr, L. C.; Harley, R. A. Modeling the Effect of Weekday–Weekend Differences in Motor Vehicle Emissions on Photochemical Air Pollution in Central California. *Environ. Sci. Technol.* **2002a**, *36*, 4099–4106.

(28) Marr, L. C.; Harley, R. A. Spectral analysis of weekday–weekend differences in ambient ozone, nitrogen oxide, and non-methane hydrocarbon time series in California. *Atmos. Environ.* **2002b**, *36*, 2327–2335.

(29) Murphy, J.; Day, D.; Cleary, P.; Wooldridge, P.; Millet, D.; Goldstein, A.; Cohen, R. The weekend effect within and downwind of Sacramento: Part 1. Observations of ozone, nitrogen oxides, and VOC reactivity. *Atmos. Chem. Phys. Discuss.* **2006**, *6*, 11427–11464.

(30) Pierce, T.; Hogrefe, C.; Trivikrama Rao, S.; Porter, P. S.; Ku, J.-Y. Dynamic evaluation of a regional air quality model: Assessing the emissions-induced weekly ozone cycle. *Atmos. Environ.* **2010**, *44*, 3583–3596.

(31) Koo, B.; Jung, J.; Pollack, A. K.; Lindhjem, C.; Jimenez, M.; Yarwood, G. Impact of meteorology and anthropogenic emissions on the local and regional ozone weekend effect in Midwestern U.S. *Atmos. Environ.* **2012**, *57*, 13–21.

(32) Ramboll. *User's Guide: Comprehensive Air quality Model with extensions, Version 6.50*. Ramboll Environment and Health. (2018). [https://camx-wp.azurewebsites.net/Files/CAMxUsersGuide\\_v6.50.pdf](https://camx-wp.azurewebsites.net/Files/CAMxUsersGuide_v6.50.pdf). Accessed 8/13/2020.

(33) U.S.EPA. *Air Quality Modeling Technical Support Document for the Regulatory Impact Analysis for the Revisions to the National Ambient Air Quality Standards for Particulate Matter*. (2012). <https://www3.epa.gov/ttn/naaqs/standards/pm/data/201212aqm.pdf>. Accessed 9/4/2020.

(34) U.S.EPA. *2016 Version 7.1 Technical Support Document*. (2019). <https://www.epa.gov/air-emissions-modeling/2016-version-71-technical-support-document>. Accessed 9/4/2020.

(35) Skamarock, W. C.; Klemp, J. B. A time-split nonhydrostatic atmospheric model for weather research and forecasting applications. *J. Comput. Phys.* **2008**, *227*, 3465–3485.

(36) U.S.EPA. (2017). *Meteorological Model Performance for Annual 2016 Simulation WRF v3.8. Research Triangle Park, NC, 27711: Office of Air Quality Planning and Standards*. [https://www.epa.gov/sites/default/files/2020-10/documents/met\\_model\\_performance-2016\\_wrf.pdf](https://www.epa.gov/sites/default/files/2020-10/documents/met_model_performance-2016_wrf.pdf). Accessed 9/4/2020.

(37) Bey, I.; Jacob, D. J.; Yantosca, R. M.; Logan, J. A.; Field, B. D.; Fiore, A. M.; Li, Q.; Liu, H. Y.; Mickley, L. J.; Schultz, M. G. Global modeling of tropospheric chemistry with assimilated meteorology: Model description and evaluation. *J. Geophys. Res.: Atmos.* **2001**, *106*, 23073–23095.

(38) Mathur, R.; Xing, J.; Gilliam, R.; Sarwar, G.; Hogrefe, C.; Pleim, J.; Pouliot, G.; Roselle, S.; Spero, T. L.; Wong, D. C.; Young, J. Extending the Community Multiscale Air Quality (CMAQ) modeling system to hemispheric scales: overview of process considerations and initial applications. *Atmos. Chem. Phys.* **2017**, *17*, 12449–12474.

(39) U.S.EPA. *Health Risk and Exposure Assessment for Ozone Final Report*. Office of Air Quality Planning and Standards: RTP, NC (Vol.

EPA-452/R-14-004a). (2014). <https://www3.epa.gov/ttn/naaqs/standards/ozone/data/20140829healthrea.pdf>. Accessed 9/4/2020.

(40) U.S.EPA. *Policy Assessment for the Review of the Ozone National Ambient Air Quality Standards*. (EPA-452/R-20-001); U.S.EPA: Research Triangle Park, NC, (2020a) Retrieved from <https://www.epa.gov/naaqs/ozone-o3-standards-policy-assessments-current-review>. Accessed 4/7/2021.

(41) Cohan, D. S.; Napelenok, S. L. Air quality response modeling for decision support. *Atmosphere* **2011**, *2*, 407–425.

(42) Napelenok, S. L.; Cohan, D. S.; Odman, M. T.; Tonse, S. Extension and evaluation of sensitivity analysis capabilities in a photochemical model. *Environ. Model. Softw.* **2008**, *23*, 994–999.

(43) Pierce, T.; Geron, C.; Bender, L.; Dennis, R.; Tonneisen, G.; Guenther, A. Influence of increased isoprene emissions on regional ozone modeling. *J. Geophys. Res.: Atmos.* **1998**, *103*, 25611–25629.

(44) de Winter, J. C. Using the Student's t-test with extremely small sample sizes. *Pract. Assess. Res. Evaluation* **2013**, *18*, 10.

(45) Simon, H.; Baker, K. R.; Akhtar, F.; Napelenok, S. L.; Possiel, N.; Wells, B.; Timin, B. A direct sensitivity approach to predict hourly ozone resulting from compliance with the National Ambient Air Quality Standard. *Environ. Sci. Technol.* **2013**, *47*, 2304–2313.

(46) Dodge, M. C. Combined use of modeling techniques and smog chamber data to derive ozone-precursor relationships. In *International conference on photochemical oxidant pollution and its control: Proceedings*; US Environmental Protection Agency, Environmental Sciences Research Laboratory: Research Triangle Park, NC, (1977), (2), 881–889.

(47) Kinosian, J. R. Ozone-precursor relationships from EKMA diagrams. *Environ. Sci. Technol.* **1982**, *16*, 880–883.

(48) Xing, J.; Wang, S. X.; Jang, C.; Zhu, Y.; Hao, J. M. Nonlinear response of ozone to precursor emission changes in China: a modeling study using response surface methodology. *Atmos. Chem. Phys.* **2011**, *11*, 5027–5044.

(49) Guo, H.; Chen, K.; Wang, P.; Hu, J.; Ying, Q.; Gao, A.; Zhang, H. Simulation of summer ozone and its sensitivity to emission changes in China. *Atmos. Pollut. Res.* **2019**, *10*, 1543–1552.

(50) Hakami, A.; Odman, M. T.; Russell, A. G. High-order, direct sensitivity analysis of multidimensional air quality models. *Environ. Sci. Technol.* **2003**, *37*, 2442–2452.

(51) Wells, B.; Dolwick, P.; Eder, B.; Evangelista, M.; Foley, K.; Mannhardt, E.; Misenis, C.; Weishampel, A. Improved estimation of trends in U.S. ozone concentrations adjusted for interannual variability in meteorological conditions. *Atmos. Environ.* **2021**, *248*, No. 118234.

(52) Choi, Y.; Souri, A. H. Chemical condition and surface ozone in large cities of Texas during the last decade: Observational evidence from OMI, CAMS, and model analysis. *Remote Sens. Environ.* **2015**, *168*, 90–101.

(53) Dye, T. S.; Roberts, P. T.; Korc, M. E. Observations of transport processes for ozone and ozone precursors during the 1991 Lake Michigan Ozone Study. *J. Appl. Meteorol. Climatol.* **1995**, *34*, 1877–1889.

(54) Foley, T.; Betterton, E. A.; Robert Jacko, P. E.; Hillery, J. Lake Michigan air quality: the 1994–2003 LADCO aircraft Project (LAP). *Atmos. Environ.* **2011**, *45*, 3192–3202.

(55) U.S.EPA. *Final Area Designations for the 2015 Ozone National Ambient Air Quality Standards Technical Support Documentation*. (2018). Retrieved from [https://www.epa.gov/sites/production/files/2018-05/documents/mi\\_tsd\\_final\\_0.pdf](https://www.epa.gov/sites/production/files/2018-05/documents/mi_tsd_final_0.pdf). Accessed 4/7/2021.

(56) Blanchard, C. L.; Tanenbaum, S.; Lawson, D. R. Differences between weekday and weekend air pollutant levels in Atlanta; Baltimore; Chicago; Dallas–Fort Worth; Denver; Houston; New York; Phoenix; Washington, DC; and surrounding areas. *J. Air Waste Manage. Assoc.* **2008**, *58*, 1598–1615.

(57) Wolff, G. T.; Kahlbaum, D. F.; Heuss, J. M. The vanishing ozone weekday/weekend effect. *J. Air Waste Manage. Assoc.* **2013**, *63*, 292–299.

(58) de Foy, B. City-level variations in NO<sub>x</sub> emissions derived from hourly monitoring data in Chicago. *Atmos. Environ.* **2018**, *176*, 128–139.

(59) Brook, J. R.; Makar, P. A.; Sills, D. M. L.; Hayden, K. L.; McLaren, R. Exploring the nature of air quality over southwestern Ontario: main findings from the Border Air Quality and Meteorology Study. *Atmos. Chem. Phys.* **2013**, *13*, 10461–10482.

(60) Makar, P. A.; Zhang, J.; Gong, W.; Stroud, C.; Sills, D.; Hayden, K. L.; Brook, J.; Levy, I.; Mihele, C.; Moran, M. D.; Tarasick, D. W.; He, H.; Plummer, D. Mass tracking for chemical analysis: the causes of ozone formation in southern Ontario during BAQS-Met 2007. *Atmos. Chem. Phys.* **2010**, *10*, 11151–11173.

(61) Nolte, C. G.; Dolwick, P. D.; Fann, N.; Horowitz, L. W.; Naik, V.; Pinder, R. W.; Spero, T. L.; Winner, D. A.; Ziska, L. H. Air Quality. In *Impacts, Risks, and Adaptation in the United States: Fourth National Climate Assessment, Volume II* [Reidmiller, D.R.; Avery, C.W.; Easterling, D.R.; Kunkel, K.E.; Lewis, K.L.M.; Maycock, T.K.; Stewart, B.C. (eds.)]. U.S. Global Change Research Program: Washington, DC, USA, 2018, 512–538.

(62) Lin, M.; Fiore, A. M.; Cooper, O. R.; Horowitz, L. W.; Langford, A. O.; Levy, H.; Johnson, B. J.; Naik, V.; Oltmans, S. J.; Senff, C. J. Springtime high surface ozone events over the western United States: Quantifying the role of stratospheric intrusions. *J. Geophys. Res.: Atmos.* (2012), *117* (D21). DOI: [10.1029/2012JD018151](https://doi.org/10.1029/2012JD018151)

(63) Vermeuel, M. P.; Novak, G. A.; Alwe, H. D.; Hughes, D. D.; Kaleel, R.; Dickens, A. F.; Kenski, D.; Czarnetzki, A. C.; Stone, E. A.; Stanier, C. O.; Pierce, R. B.; Millet, D. B.; Bertram, T. H. Sensitivity of ozone production to NO<sub>x</sub> and VOC along the lake Michigan coastline. *J. Geophys. Res.: Atmos.* **2019**, *124*, 10989–11006.

(64) He, H.; Liang, X.-Z.; Sun, C.; Tao, Z.; Tong, D. Q. The long-term trend and production sensitivity change in the U.S. ozone pollution from observations and model simulations. *Atmos. Chem. Phys.* **2020**, *20*, 3191–3208.

(65) TCEQ *Revisions to the State Implementation Plan (SIP) for the Control of Ozone Air Pollution Houston/Galveston Ozone*; Texas Commission on Environmental Quality: Austin, TX (Project No. 2004–042-SIP-NR). 2004. <https://www.tceq.texas.gov/airquality/sip/sipplans.html>. Accessed 11/10/2021.

(66) TCEQ *Revisions to the State of Texas Air Quality Implementation Plan for the Control of Ozone Air Pollution: Houston-Galveston-Brazoria1997 Eight-Hour Ozone Standard Nonattainment Area*; Texas Commission on Environmental Quality: Austin, TX (Project No. 2012–002-SIP-NR). 2013. <https://www.tceq.texas.gov/airquality/sip/sipplans.html>. Accessed 11/10/2021.

(67) U.S.EPA. *Reclassification of Major Sources as Area Sources Under Section 112 of the Clean Air Act*. (224); Federal Register: (2020b). Retrieved from <https://www.govinfo.gov/content/pkg/FR-2020-11-19/pdf/2020-22044.pdf>. Accessed 4/7/2021.

(68) Pye, H. O. T.; Pouliot, G. A. Modeling the role of alkanes, polycyclic aromatic hydrocarbons, and their oligomers in secondary organic aerosol formation. *Environ. Sci. Technol.* **2012**, *46*, 6041–6047.